



# Further Enhancements to the High Frequency Target Strength Prediction Capabilities of AVAST

*D.P. Brennan  
Martec Limited*

*Martec Limited  
1888 Brunswick Street, Suite 400  
Halifax, Nova Scotia  
B3J 3J8*

*Contract Number: W7707-03-2334*

*Contract Scientific Authority: L.E. Gilroy, 902-426-3100 x365*

## Defence R&D Canada – Atlantic

Contract Report  
DRDC Atlantic CR 2007-216  
August 2007

This page intentionally left blank.

# **Further Enhancements to the High Frequency Target Strength Prediction Capabilities of AVAST**

D.P. Brennan  
Martec Limited

Martec Limited  
1888 Brunswick Street, Suite 400  
Halifax, Nova Scotia  
B3J 3J8

Contract number: W7707-03-2334

Contract Scientific Authority: L.E. Gilroy, 902-426-3100 x365

**Defence R&D Canada – Atlantic**

**Contract Report**

DRDC Atlantic CR 2007-216

August 2007

Scientific Authority

*Original signed by Layton Gilroy*

---

Layton Gilroy

Approved by

*Original signed by David Hopkin*

---

David Hopkin

Head, Maritime Asset Protection

Approved for release by

*Original signed by James L Kennedy*

---

James L Kennedy

DRP Chair

Disclaimer

The scientific or technical validity of this Contract Report is entirely the responsibility of the contractor and the contents do not necessarily have the approval or endorsement of Defence R&D Canada.

© Her Majesty the Queen as represented by the Minister of National Defence, 2007

© Sa majesté la reine, représentée par le ministre de la Défense nationale, 2007

## **Abstract**

---

The development and incorporation of the latest enhancements to the AVAST code are described. The purpose of this work was to make the modeling of the physical environment more realistic, while ensuring that the code runs as efficiently as possible. To this end several new features have been added. These include modifying the high-frequency Kirchhoff scattering method in order to allow for at least one reflection and upgrading the existing boundary element surface panel integration routines. The contract also addresses the need to investigate the high frequency target strength of Manta shapes.

## **Résumé**

---

L'élaboration et l'intégration des améliorations les plus récentes apportées au logiciel AVAST sont décrites dans le présent document. Le but des travaux était de modéliser le milieu physique de manière plus réaliste, tout en veillant à ce que le logiciel soit exécuté le plus efficacement possible. À cette fin, de nouveaux attributs y ont été ajoutés. Ils consistent à modifier la méthode de diffusion de Kirchhoff pour les hautes fréquences de façon à permettre au moins une réflexion et à améliorer les routines actuelles d'intégration des panneaux de surface par éléments de frontière. Le contrat porte également sur l'étude de l'indice de réflexion à haute fréquence des mines Manta.

This page intentionally left blank.

# Executive summary

---

## Introduction

Work by DRDC and Martec in underwater/structural acoustics has resulted in the development of a series of computer programs, collectively named AVAST, for the numerical prediction of the acoustic radiation and scattering from floating or submerged elastic structures immersed in either infinite, half-space or finite-depth fluid domains. AVAST combines both the finite element method for the structure and the boundary integral equation technique for the fluid. The finite element method is used to predict the natural frequencies and related mode shapes of the structure in-vacuo. The boundary integral equation method is used to generate a system of equations relating structural displacements to fluid acoustic pressures. In an attempt to make the modeling of sound radiated and scattered from structures more realistic, several enhancements were incorporated into the existing AVAST suite. These include modifying the high-frequency Kirchhoff scattering method to allow for at least one reflection and upgrading the existing boundary element surface panel integration routines. This report also includes a summary of a series of AVAST elastic target strength analysis conducted on Manta-like mine models.

## Results

The AVAST software was upgraded to allow for the prediction of high frequency target strengths of underwater targets in shallow water, to include the effects of multiple scatterers and secondary reflections, and to allow for modelling of thin bodies. A realistic examination of the target strength of a Manta-like mine was also performed demonstrating the increased target echo strength at frequencies close to the structural resonant frequencies (when submerged).

## Significance

This upgraded version of AVAST will be used to improve the accuracy of target echo strength predictions of all underwater targets and the results from the mine investigation will be used to compare with other measured or predicted data when available to assess the accuracy of the AVAST software for this class of problems.

## Future plans

The improved AVAST will be used to assess the acoustic target strength of CF submarines and the elastic target strength of other mine-like targets.

Brennan, D.P. 2007. Further Enhancements to the High Frequency Target Strength Prediction Capabilities of AVAST. DRDC Atlantic CR 2007-216. DRDC Atlantic.

# Sommaire

---

## Introduction

Le programme de recherche en collaboration entre RDDC et Martec sur l'acoustique sous marine (structures immergées) a donné lieu à l'élaboration d'une série de logiciels, regroupés sous l'appellation AVAST, permettant de calculer le rayonnement acoustique et la diffusion du rayonnement par des structures élastiques flottantes ou immergées dans un fluide infini, ou finie, occupant un demi espace ou un volume défini. Le logiciel AVAST conjugue la méthode des éléments finis (MEF), pour la structure, et la méthode des équations intégrales de frontière, pour le fluide. La méthode des éléments finis (MEF) sert à prévoir les fréquences naturelles et les formes connexes de la structure in vacuo. La méthode des équations intégrales de frontière sert à produire un système d'équations qui relie les déplacements structuraux aux pressions acoustiques du fluide.

Dans le but de rendre la modélisation du son émis et diffusé par les structures plus réaliste, on a récemment apporté plusieurs améliorations à la suite AVAST. Celles ci consistaient notamment à améliorer la méthode de diffusion de Kirchhoff pour les hautes fréquences afin de tenir compte d'au moins une réflexion, et à améliorer les routines actuelles d'intégration des panneaux de surface par éléments de frontière. Le rapport comprend également le résumé d'une série d'analyses de l'indice de réflexion par des cibles élastiques réalisées sur des modèles semblables aux mines Manta, à l'aide du programme AVAST.

## Résultats

Le logiciel AVAST a été amélioré afin de calculer l'indice de réflexion des cibles émettrices de hautes fréquences en eaux peu profondes, en vue de tenir compte des effets des diffusions multiples et des réflexions secondaires et de permettre la modélisation des structures minces. Un examen réaliste de l'indice de réflexion des cibles semblables aux mines Manta a également été réalisé dans le but de démontrer que l'amplitude de l'écho des cibles est plus grande à des fréquences proches de la fréquence de résonance de la structure (cibles immergées).

## Portée

La version améliorée du programme AVAST permettra d'améliorer l'exactitude des calculs de l'amplitude de l'écho de toutes les cibles sous marines, et les résultats de l'étude sur les mines seront utilisés pour comparer ces prévisions avec d'autres données mesurées ou calculées lorsqu'elles seront disponibles, dans le but d'évaluer la pertinence de l'utilisation du logiciel AVAST pour la résolution de ce type de problèmes.

## Recherches futures

Le programme AVAST amélioré sera utilisé pour évaluer l'indice de réflexion acoustique des sous marins des FC et l'indice de réflexion d'autres cibles élastiques semblables à des mines.

Brennan, D.P. 2007. Further Enhancements to the High Frequency Target Strength Prediction Capabilities of AVAST. DRDC Atlantic CR 2007-216. DRDC Atlantic.

# Table of contents

---

Abstract.....	i
Executive summary .....	iii
Sommaire.....	iv
Table of contents .....	v
List of figures .....	vi
1. Introduction .....	1
2. Manta Shape Target Strength Analysis .....	2
2.1 Structural Modeling.....	2
2.2 Boundary Element Modeling .....	2
2.3 Results .....	3
2.4 Target Strength Predictions .....	3
3. Upgrade the AVAST Boundary Element Surface Panel Integration Routines .....	30
4. Upgrade Kirchhoff Scattering Capability .....	31
4.1 Free Surface – Shallow Water Effects.....	31
4.2 Multiple Reflections .....	32
4.3 Example.....	32
5. References .....	35
Distribution list.....	37

## List of figures

---

Figure 2.1 Schematic Showing Overall Dimensions of Manta Shape.....	5
Figure 2.2 . Finite Element Mesh of Manta Shape with Quarter Cut Out to Show Core Structure .....	5
Figure 2.3 . Wet Mode 7.....	6
Figure 2.4 . Wet Mode 7.....	6
Figure 2.5 . Wet Mode 8.....	7
Figure 2.6 . Wet Mode 10.....	7
Figure 2.7 . Wet Mode 10.....	8
Figure 2.8 . Wet Mode 13.....	8
Figure 2.9 . Wet Mode 15.....	9
Figure 2.10 . Wet Mode 17.....	9
Figure 2.11 . Wet Mode 19.....	10
Figure 2.12 . Wet Mode 25.....	10
Figure 2.13 . Wet Mode 25.....	11
Figure 2.14 . Wet Mode 27.....	11
Figure 2.15 . Wet Mode 27.....	12
Figure 2.16 . Wet Mode 29.....	12
Figure 2.17 . Manta_365Hz_0e-3Damping .....	13
Figure 2.18 . Manta_379Hz_0e-3Damping .....	13
Figure 2.19 . Manta_396Hz_0e-3Damping .....	14
Figure 2.20 . Manta_419Hz_0e-3Damping .....	14
Figure 2.21 . :Manta_434Hz_0e-3Damping.....	15
Figure 2.22 . Manta_434Hz_1e-3Damping .....	15

Figure 2.23 . Manta_434Hz_2e-3Damping .....	16
Figure 2.24 . Manta_434Hz_5e-3Damping .....	16
Figure 2.25 . Manta_532Hz_0e-3Damping .....	17
Figure 2.26 . Manta_545Hz_0e-3Damping .....	17
Figure 2.27 . Manta_615Hz_0e-3Damping .....	18
Figure 2.28 . Manta_660Hz_0e-3Damping .....	18
Figure 2.29 . Manta_699Hz_0e-3Damping .....	19
Figure 2.30 . Manta_895Hz_0e-3Damping .....	19
Figure 2.31 . Manta_900Hz_0e-3Damping .....	20
Figure 2.32 . Manta_365Hz_0e-3Damping.RAT .....	20
Figure 2.33 . Manta_379Hz_0e-3Damping.RAT .....	21
Figure 2.34 . Manta_396Hz_0e-3Damping.RAT .....	21
Figure 2.35 . Manta_419Hz_0e-3Damping.RAT .....	22
Figure 2.36 . Manta_434Hz_2e-3Damping.RAT .....	22
Figure 2.37 . Manta_434Hz_5e-3Damping.RAT .....	23
Figure 2.38 . Manta_532Hz_0e-3Damping.RAT .....	23
Figure 2.39 . Manta_545Hz_0e-3Damping.RAT .....	24
Figure 2.40 . Manta_615Hz_0e-3Damping.RAT .....	24
Figure 2.41 . Manta_660Hz_0e-3Damping.RAT .....	25
Figure 2.42 . Manta_699Hz_0e-3Damping.RAT .....	25
Figure 2.43 . Manta_895Hz_0e-3Damping.RAT .....	26
Figure 2.44 . Manta_900Hz_0e-3Damping.RAT .....	26
Figure 2.45 . Manta Shape Monostatic Elastic Target Strength at 379 Hz.....	27
Figure 2.46 . Manta Shape Monostatic Elastic Target Strength at 419 Hz.....	27
Figure 2.47 . Manta Shape Monostatic Elastic Target Strength at 616 Hz.....	28

Figure 2.48 . Manta Shape Monostatic Elastic Target Strength at 660 Hz..... 28

Figure 2.49 . Manta Shape Monostatic Elastic Target Strength at 699 Hz..... 29

Figure 2.50 . Manta Shape Monostatic Elastic Target Strength at 900 Hz..... 29

Figure 3.1 . Sample Boundary Element Mesh for a Ship Hull ..... 30

Figure 4.1. Generic Submarine Sail Model ..... 33

Figure 4.2. A Comparison of Target Strength Predictions for Submarine Sail at 4 kHz (infinite Fluid vs a Free Surface Height 3m Above the Top of the Sail) ..... 34

# 1. Introduction

---

Phases one through fourteen of the DRDC/Martec collaborative research in underwater/ structural acoustics has resulted in the development of a series of computer programs, collectively named AVAST, for the numerical prediction of the acoustic radiation and scattering from floating or submerged elastic structures immersed in either infinite, half-space or finite depth fluid domains. AVAST combines both the finite element method (FEM) for the structure and the boundary integral equation technique for the fluid. The finite element method is used to predict the natural frequencies and related mode shapes of the structure in-vacuo. The boundary integral equation method (BIEM) is used to generate a system of equations relating structural displacements to fluid acoustic pressures.

In an attempt to make the modeling of sound radiated and scattered from structures more realistic, several enhancements have recently been incorporated into the previously existing AVAST suite. These include modifying the high-frequency Kirchhoff scattering method in order to allow for at least one reflection and upgrading the existing boundary element surface panel integration routines.

In the discussion which follows, details concerning the development and incorporation of these latest enhancements to the AVAST suite will be presented. Also included in this report is a summary of a series of AVAST elastic target strength analysis conducted on Manta-shaped mine models.

## 2. Manta Shape Target Strength Analysis

---

The basic geometry of the Manta shape is displayed in Figure 2.1. The larger radius of the shape is 1000mm and the smaller radius is 500mm. The shape is 375mm in height. The shape was modeled using 4-node quadratic elements and the mesh used is shown in Figure 2.2. Figure 2.2 also shows the interior of the shape with the core section modeled. The outer shell of the shape was assumed to be a composite material with a thickness of 20mm. The core and the bottom plate were assumed to be steel. The light blue elements represent the steel portions of the shape and the brown elements represent the composite sections. For simplicity, the composite was modeled as an isotropic material with a density of 2500kg/m<sup>3</sup>, an elastic modulus of 40GPa and Poisson's ratio of 0.35. The steel elements were assigned a density of 7900 kg/m<sup>3</sup>, an elastic modulus of 207GPa and Poisson's ratio of 0.30.

### 2.1 Structural Modeling

The algorithm used in AVAST for computing the elastic target strength is based on a dry-mode wet-mode approach, i.e., the dry (in-vacuo) modes of the structure are used to predict the submerged elastic response. For the purposes of this analysis, a finite element model was created based on the description provided above and a series of dry structural modes were computed using the VAST finite element code. The finite element model had a total of 21084 degrees of freedom with a total of 30 modes computed. The results of the natural frequency run are provided below in Table 2.1. Note that for the purposes of this analysis, the mine was modeled as a free-free system (no boundary constraints).

### 2.2 Boundary Element Modeling

The boundary element model used to represent the Manta shape is represented below in Figure 2.1 (using the surface panels only) and represents the wetted surface of the structure. A total of 2552 quadrilateral surface panels were used. Field points (for calculating the target strength) were located at a distance of 100 meters from the center of the shape and at a height of 165 millimeters above the sea floor (the sea floor was represented as a rigid plane). The acoustic source used to excite the shape was located at a distance of 1000 meters and a height of 165 mm above the sea floor. The wet natural frequencies computed by AVAST are provided below in Table 2.2 and the resulting mode shapes are shown in Figures 2.3-2.16.

Dry Mine Modes		Wet Mine Modes	
Mode Number	Frequency (Hz)	Mode Number	Frequency (Hz)
7	188	7	347
8	398	8	440
10	457	10	475
11	521	13	526
13	639	15	643
15	658	17	663
17	722	19	750
19	745	25	803
21	769	27	991
23	787	29	1005
25	795		
27	904		
28	983		
30	1034		

## 2.3 Results

In order to study the effects of structural elasticity on the target strength of the Manta shape, results were computed for narrow 8 Hz frequency bands approximately centered on the wet natural frequencies of the structure. Figures 2.17 – 2.31 provide plots of the radiated component of the acoustic pressure generated by a unit (1.0 Pa) incident source with various damping factors used (from 0.0 to 0.5%). The horizontal axis represents frequency while the vertical axis represents field point position in degrees (one complete rotation). These plots clearly show significant changes in the radiated pressure at the frequency approaches a coupled resonance. In a second series of figures (see Figures 2.32 – 2.44), plots representing the ratio of radiated to scattered acoustic pressure are provided. Once again, these plots clearly show a significant increase in the radiated (i.e., elastic contribution) pressure in narrow frequency bands close to coupled resonances.

## 2.4 Target Strength Predictions

In order to compute the elastic target strength, the formula used to compute the rigid target strength was modified to include the radiated, or elastic, acoustic pressure, i.e.,

$$TS_{Elastic} = 20 \text{Log}_{10} \left( \frac{\phi_{Rad} + \phi_{Scat}}{\phi_i} \right) + 20 \text{Log}_{10} (R)$$

where  $\phi_{Scat}$  represents the scattering field pressure  $\phi_{Rad}$  represents the radiated field pressure,  $\phi_i$  represents the incident pressure computed at the acoustic center (i.e., center of the mine), and R represents the distance from the acoustic center to the field points (i.e., 100 meters).

Monostatic elastic target strength results for a few select frequencies are provided below in Figures 2.45-2.50. The horizontal axis is the circumferential direction around the mine shape.

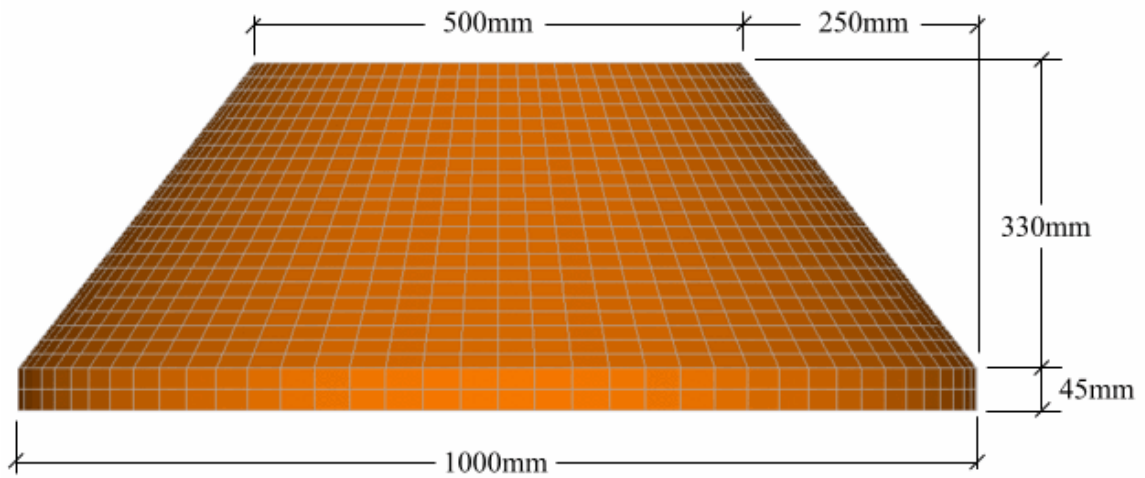


**Figure 2.1 . Schematic Showing Overall Dimensions of Manta Shape**

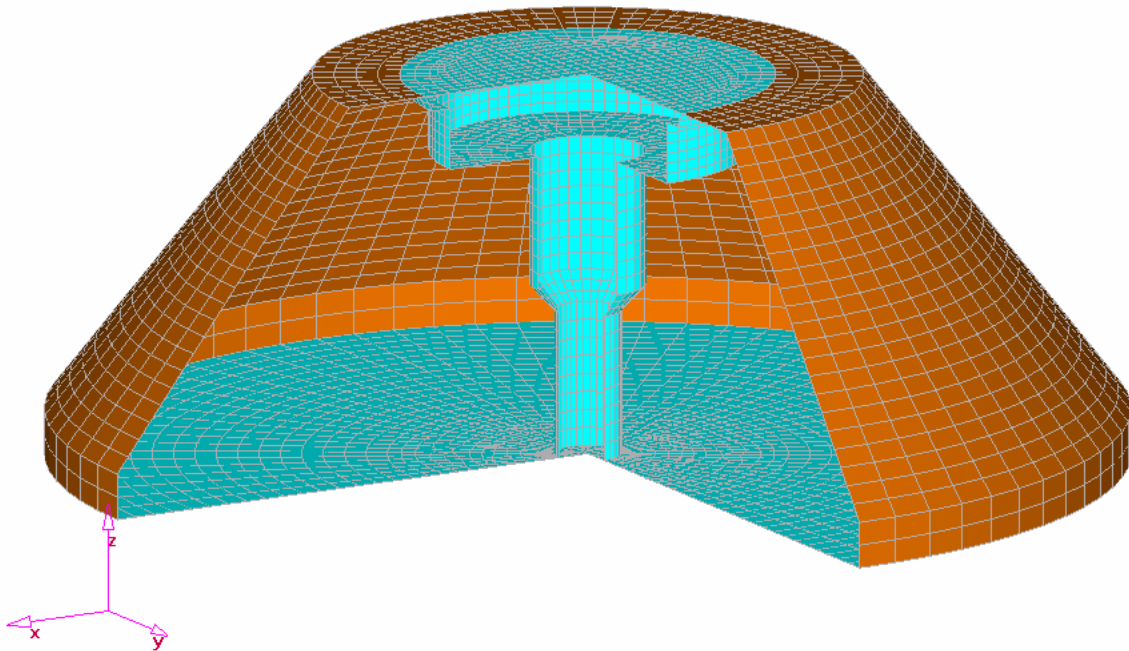


**Figure 2.2 . Finite Element Mesh of Manta Shape with Quarter Cut Out to Show Core Structure**

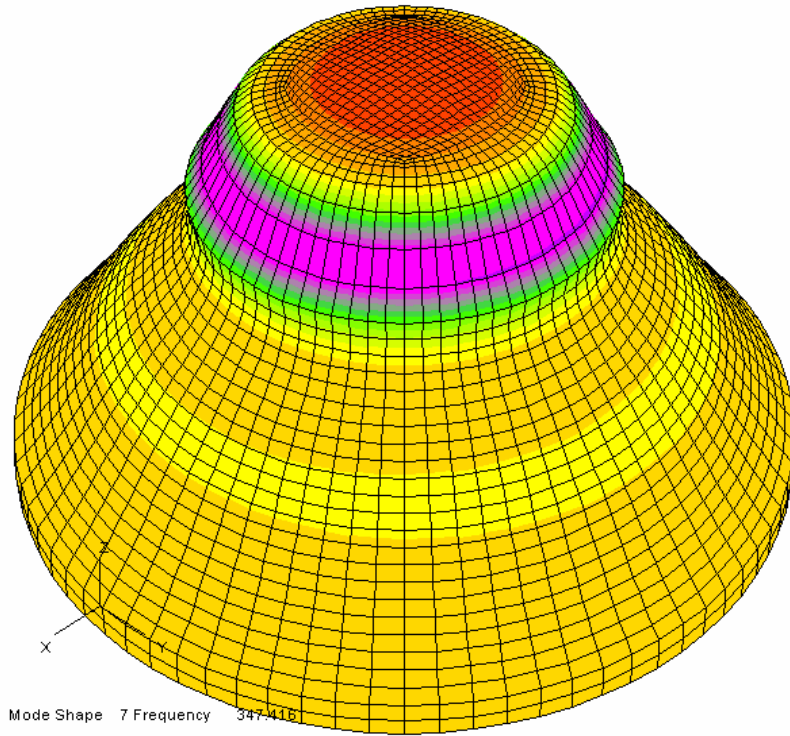


**Figure 2.3 . Wet Mode 7**

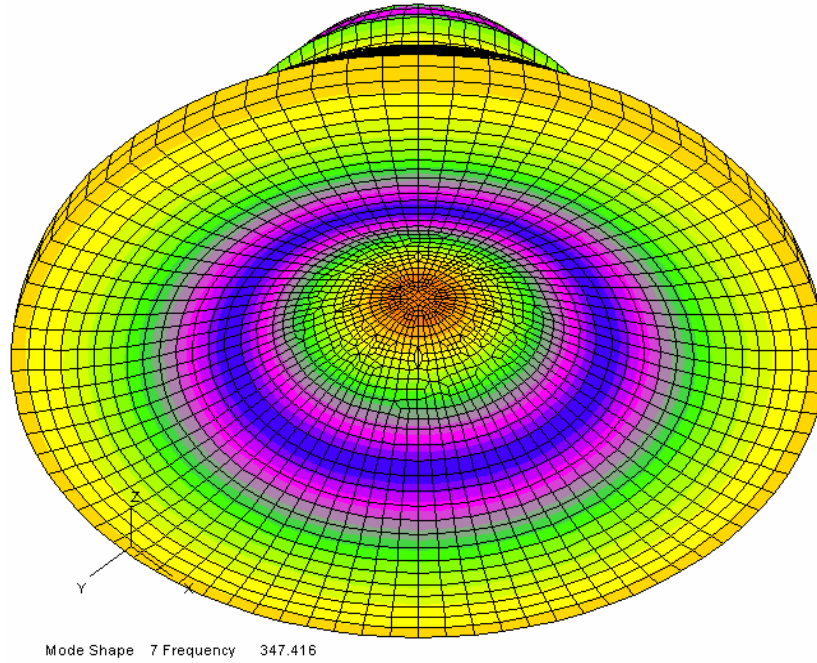
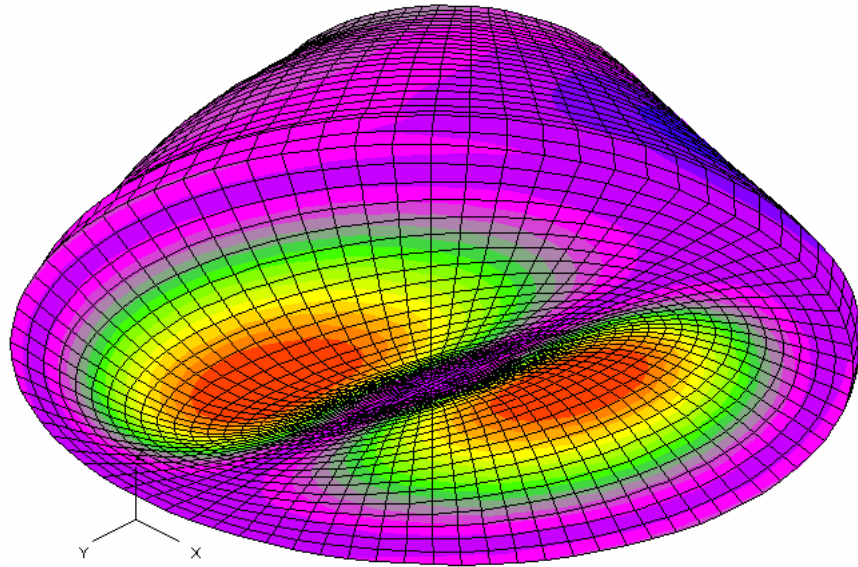
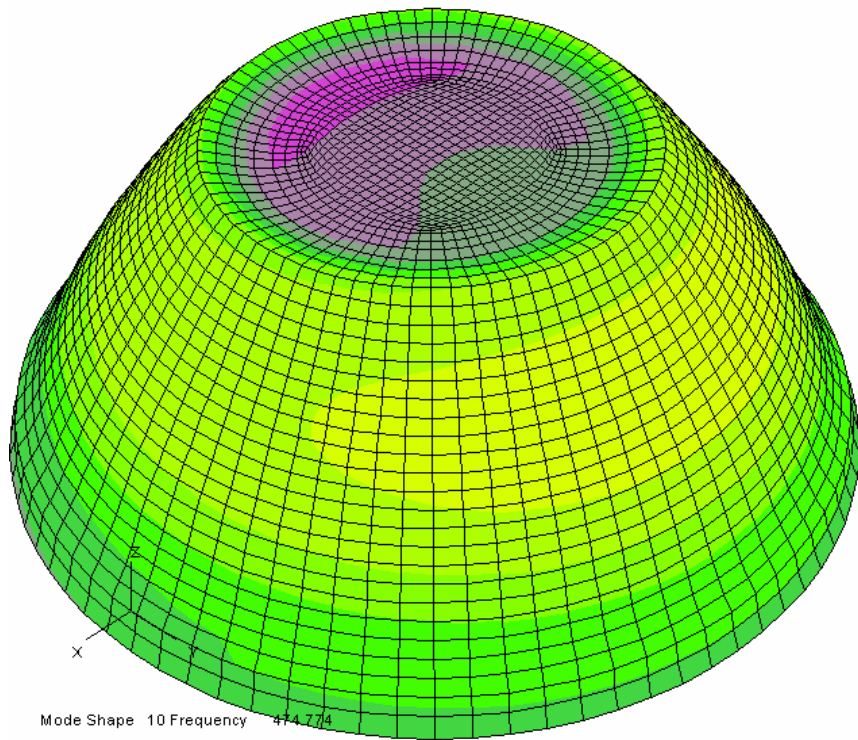


**Figure 2.4 . Wet Mode 7**



Mode Shape 8 Frequency 440.015

**Figure 2.5 . Wet Mode 8**



Mode Shape 10 Frequency 474.774

**Figure 2.6 . Wet Mode 10**

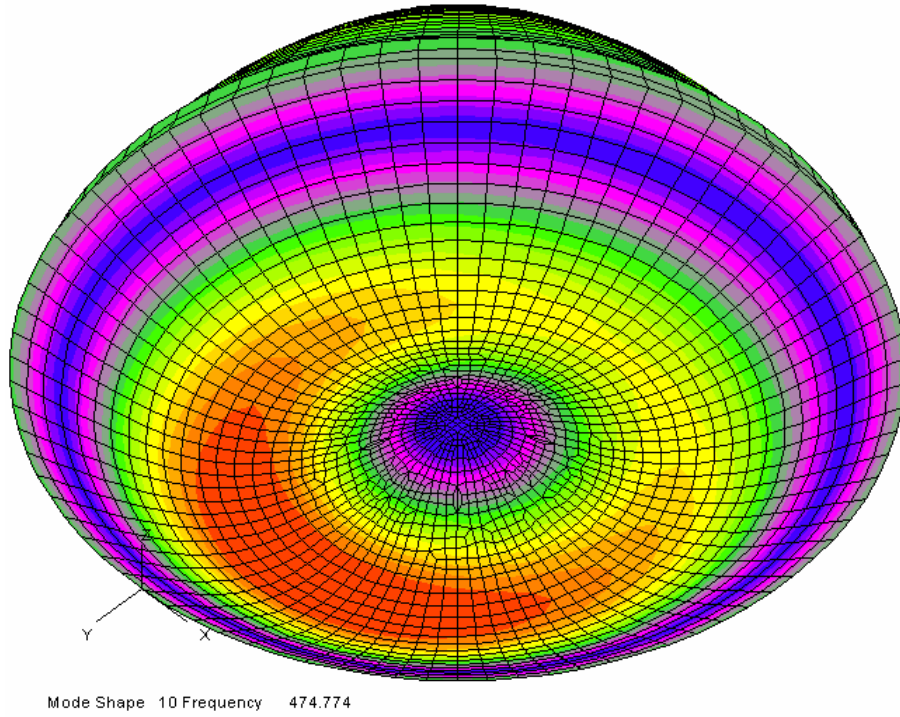


**Figure 2.7 . Wet Mode 10**

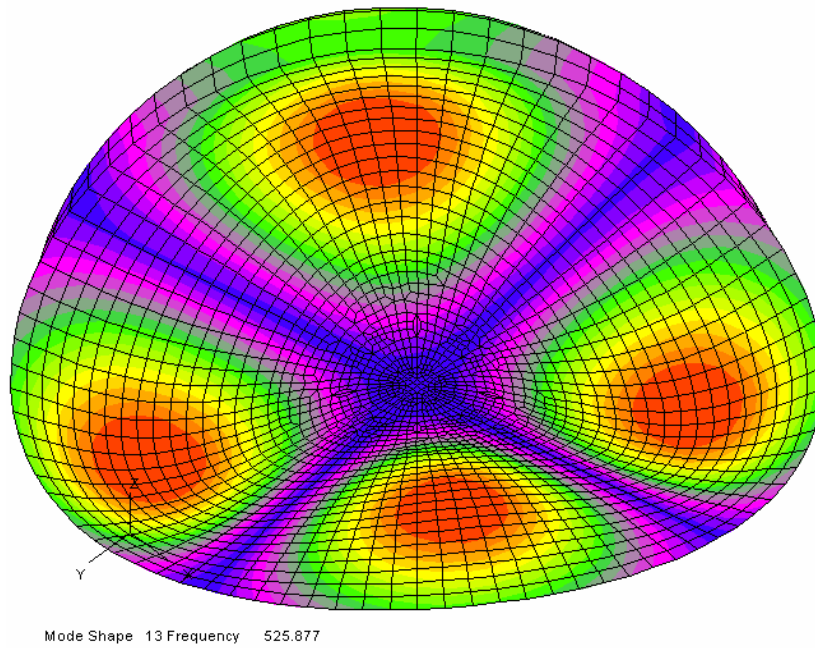


**Figure 2.8 . Wet Mode 13**

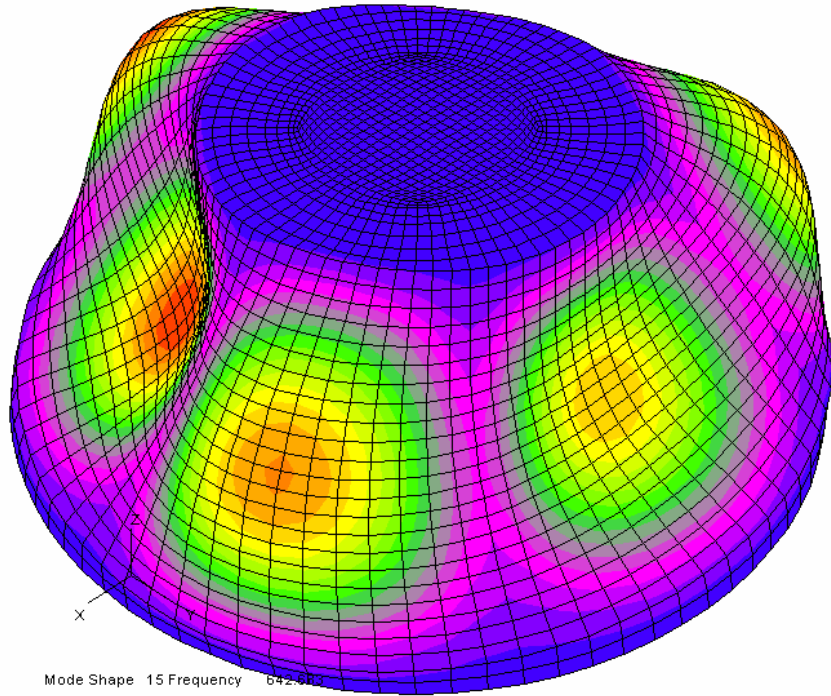


**Figure 2.9 . Wet Mode 15**

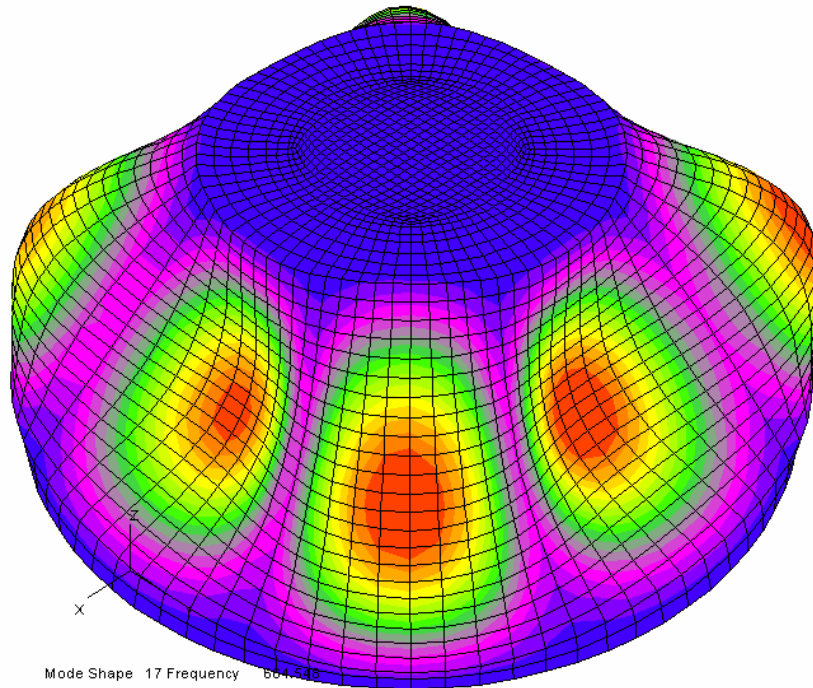


**Figure 2.10 . Wet Mode 17**

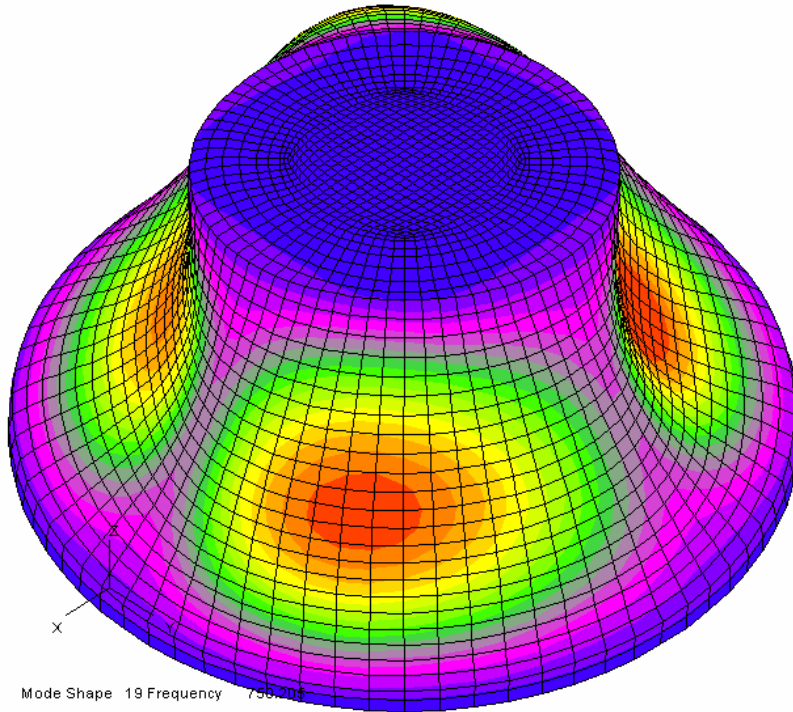


**Figure 2.11 . Wet Mode 19**

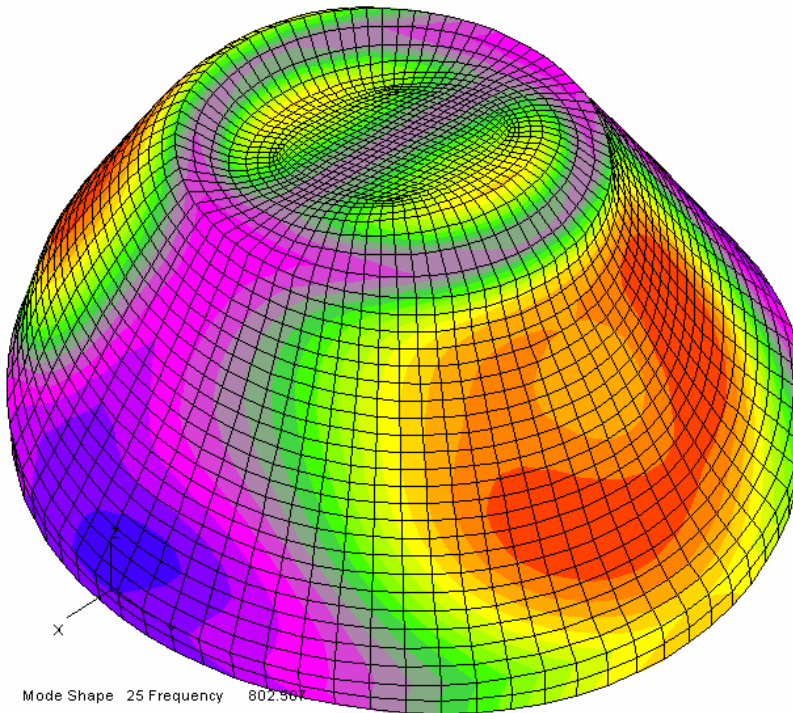


**Figure 2.12 . Wet Mode 25**

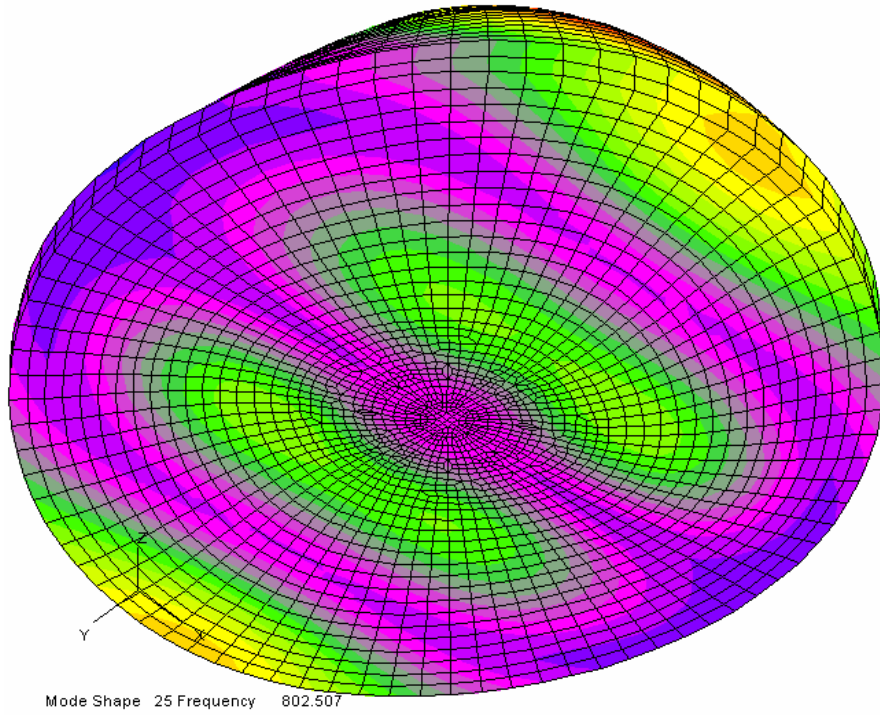


**Figure 2.13 . Wet Mode 25**

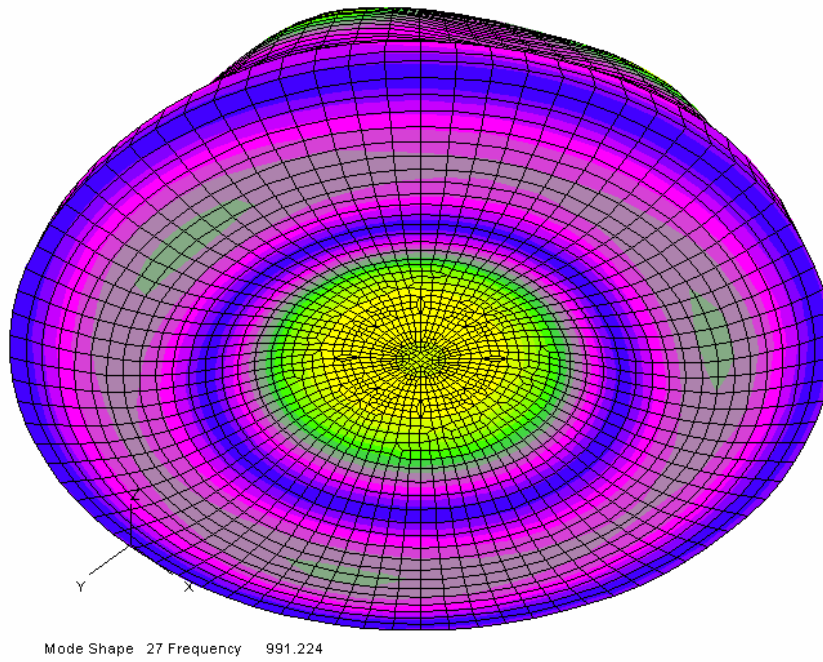


**Figure 2.14 . Wet Mode 27**

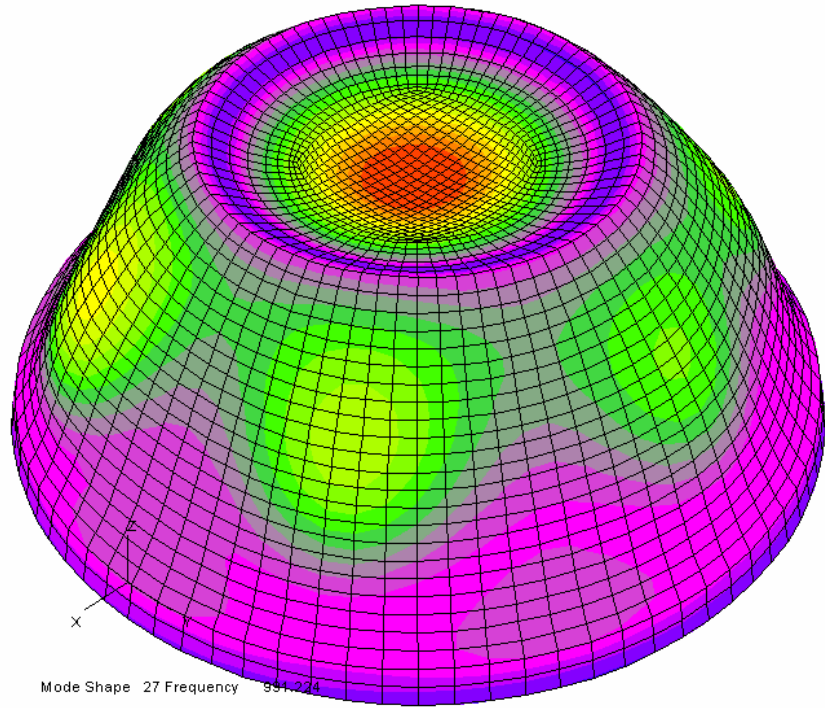


**Figure 2.15 . Wet Mode 27**

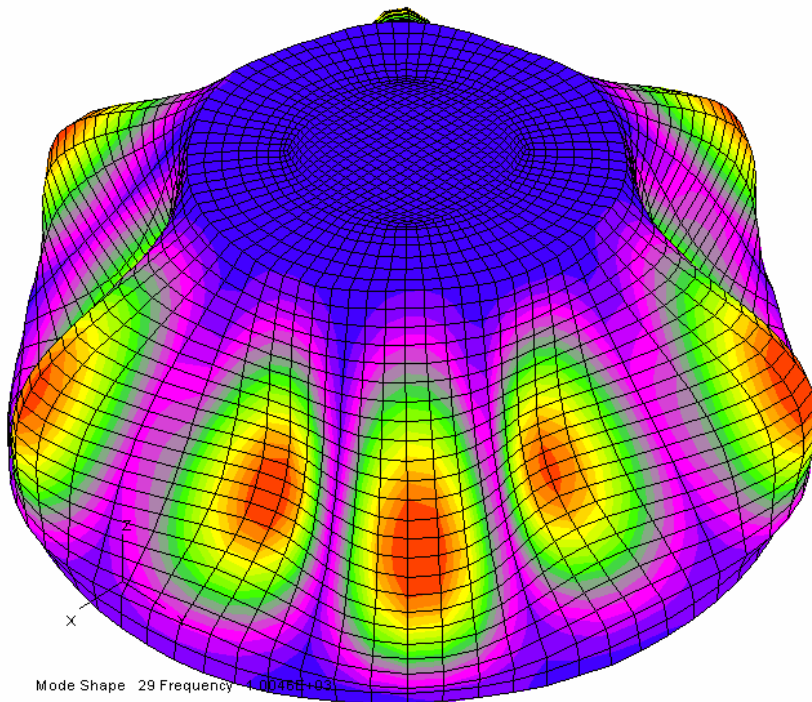


**Figure 2.16 . Wet Mode 29**

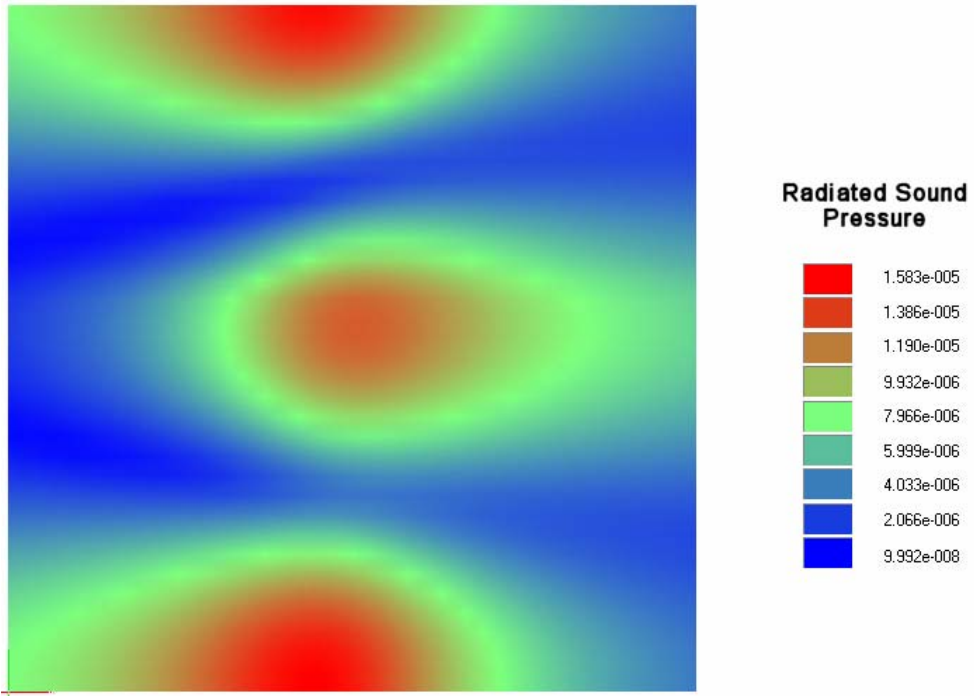


**Figure 2.17 . Manta\_365Hz\_0e-3Damping**

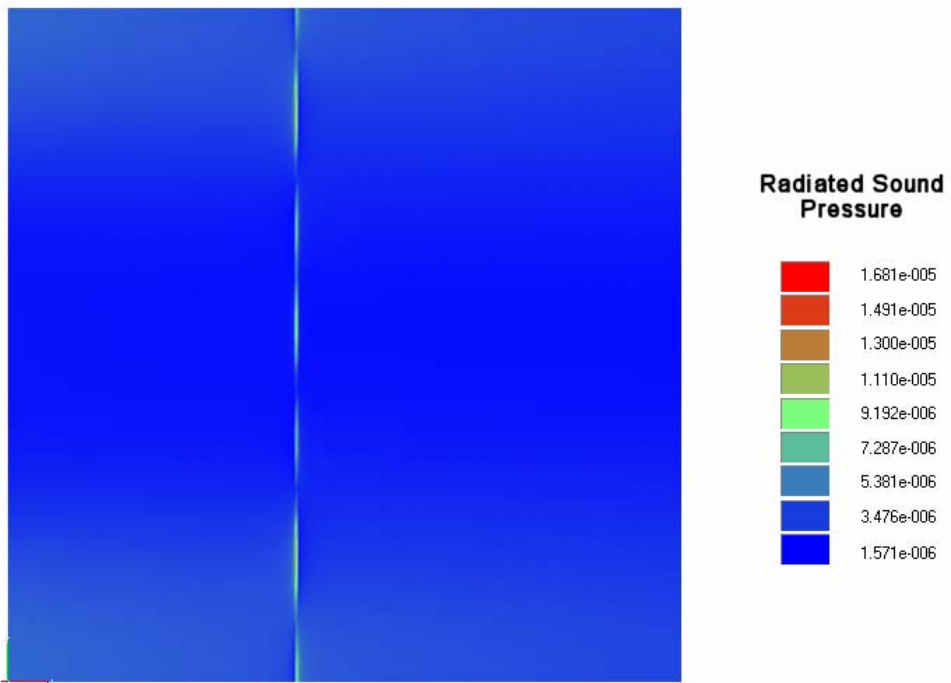


**Figure 2.18 . Manta\_379Hz\_0e-3Damping**

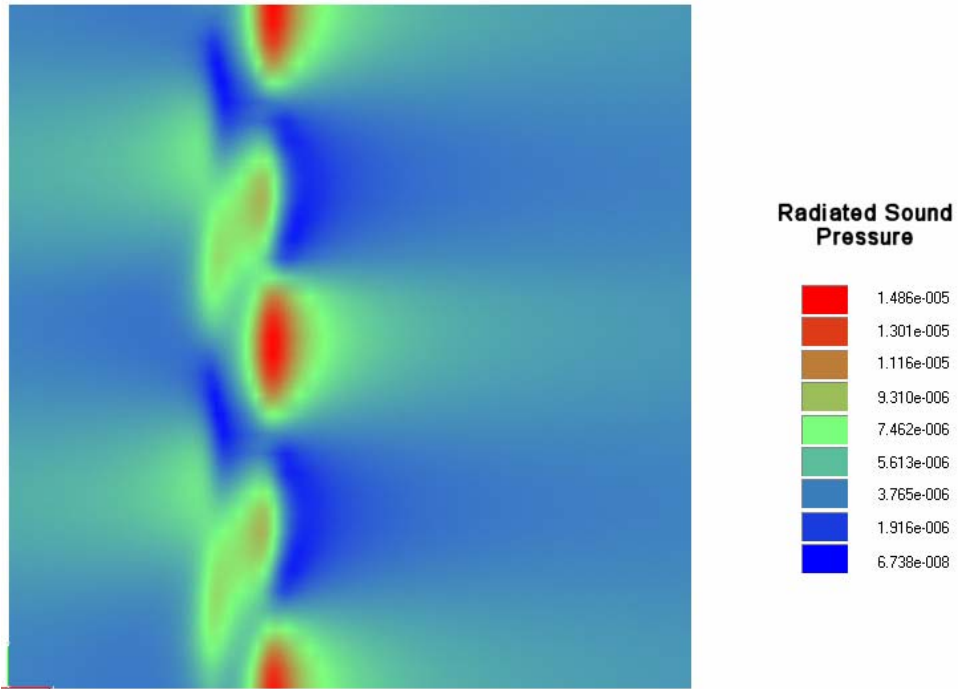


*Figure 2.19 . Manta\_396Hz\_0e-3Damping*

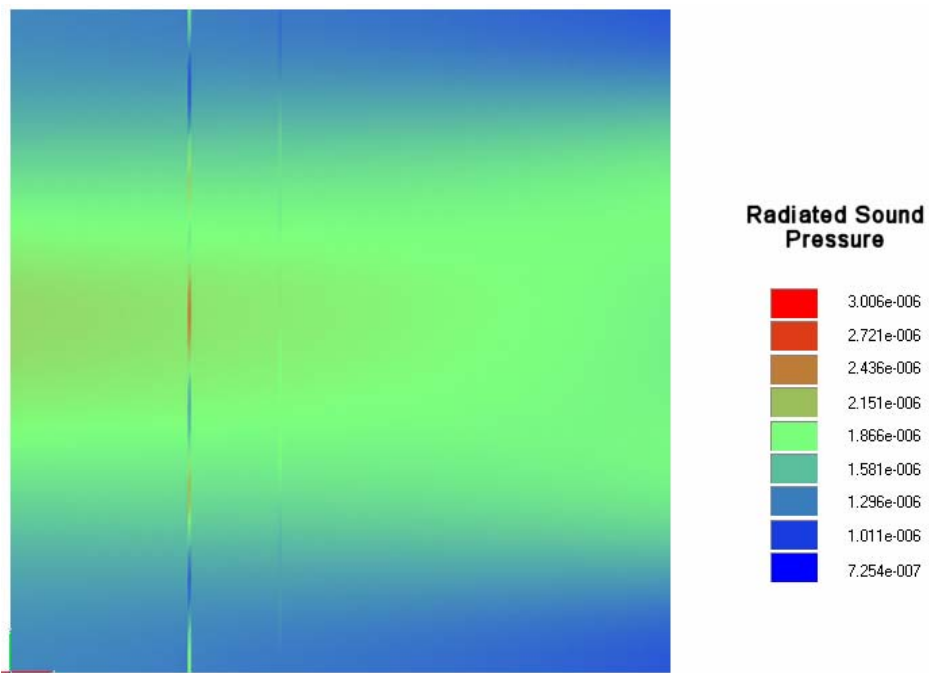


*Figure 2.20 . Manta\_419Hz\_0e-3Damping*

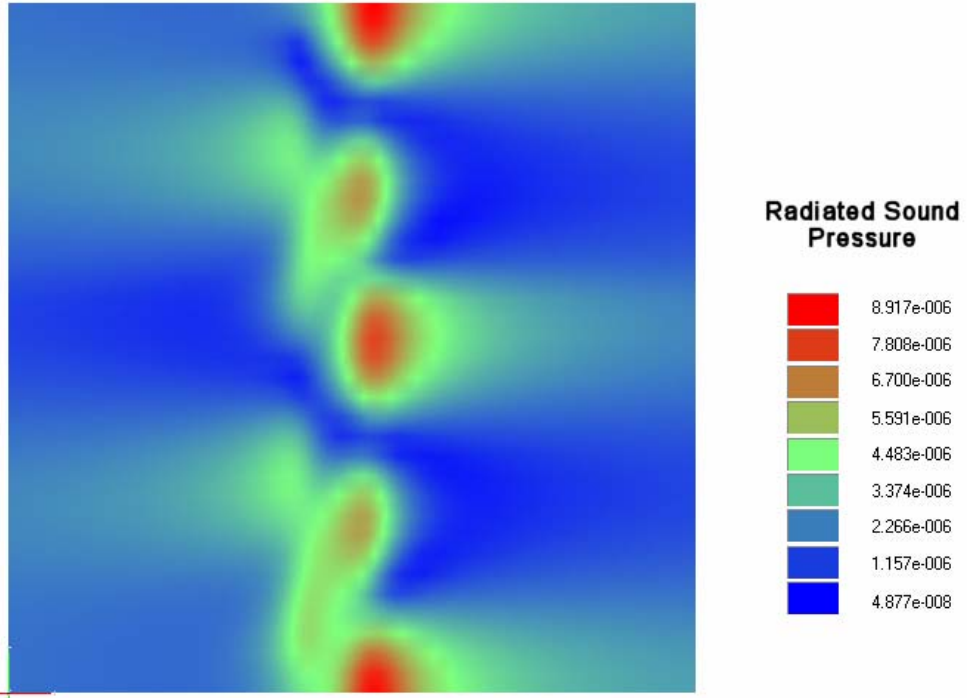


*Figure 2.21 . Manta\_434Hz\_0e-3Damping*

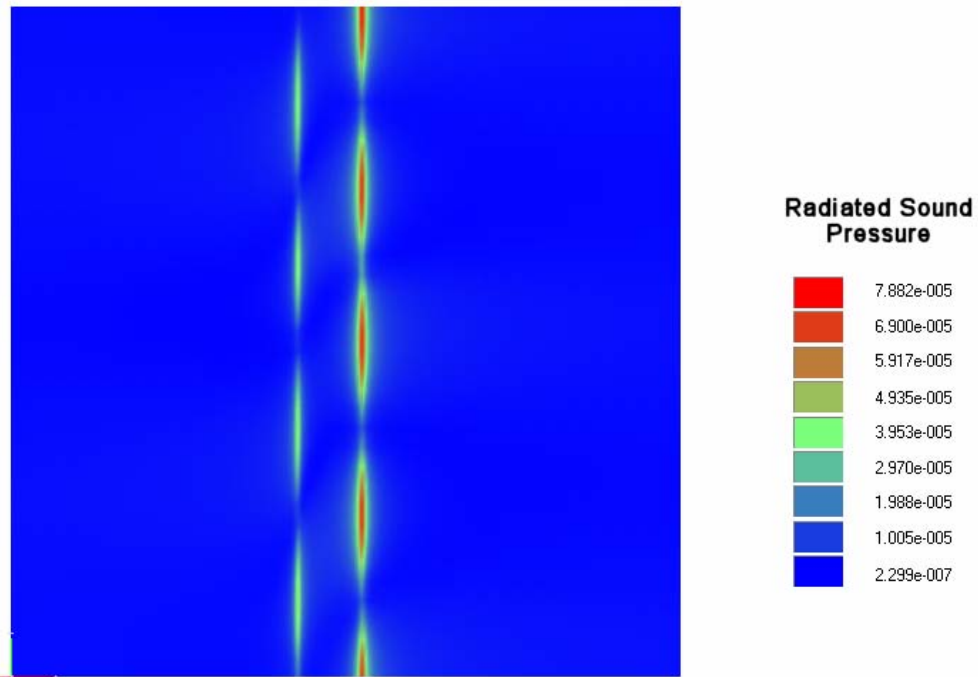


*Figure 2.22 . Manta\_434Hz\_1e-3Damping*

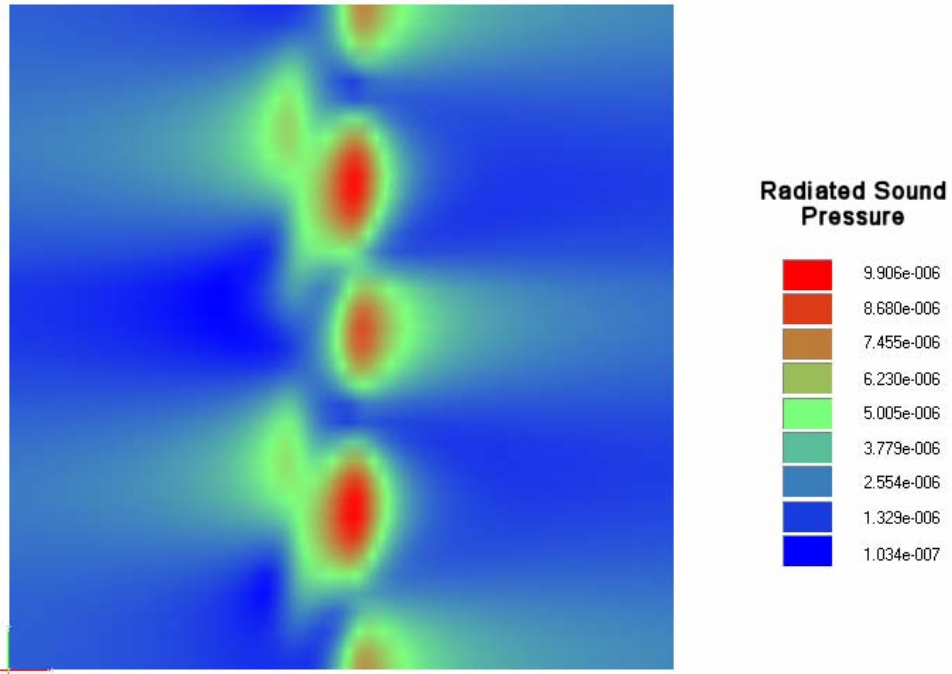


*Figure 2.23 . Manta\_434Hz\_2e-3Damping*

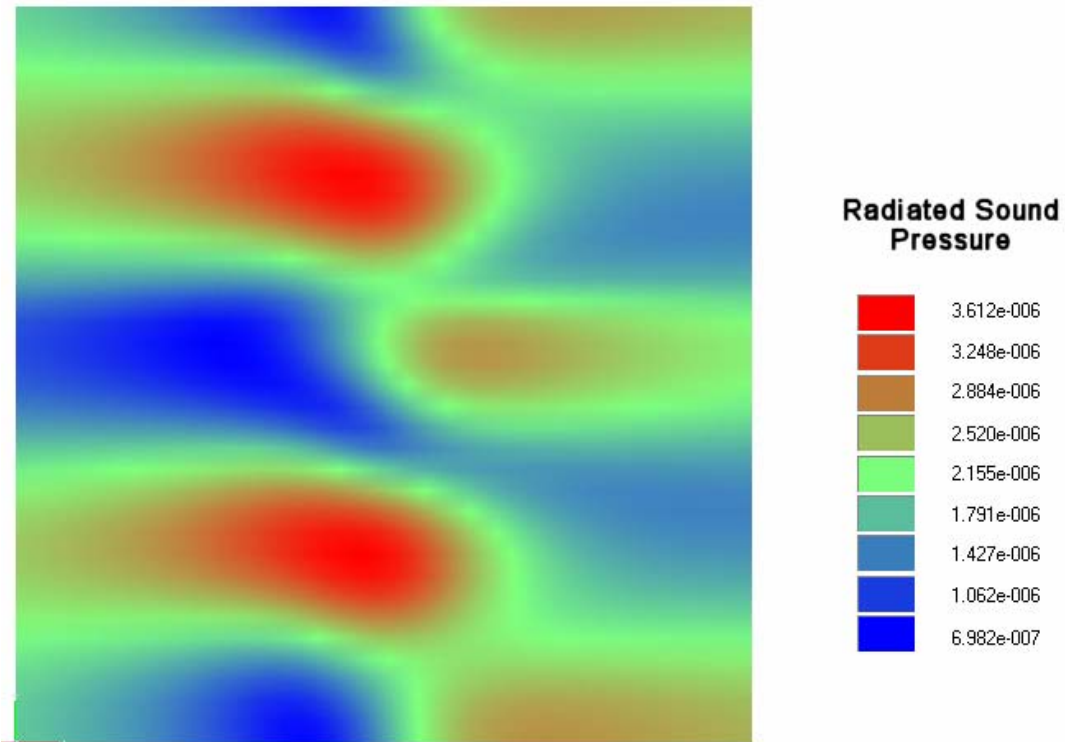


*Figure 2.24 . Manta\_434Hz\_5e-3Damping*

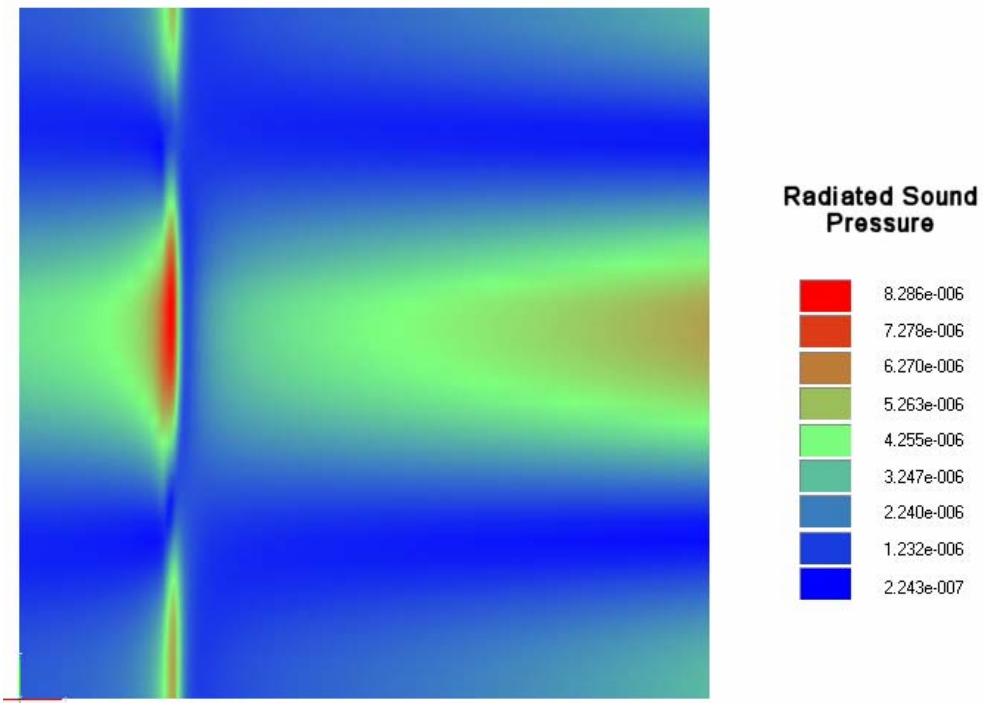


*Figure 2.25 . Manta\_532Hz\_0e-3Damping*

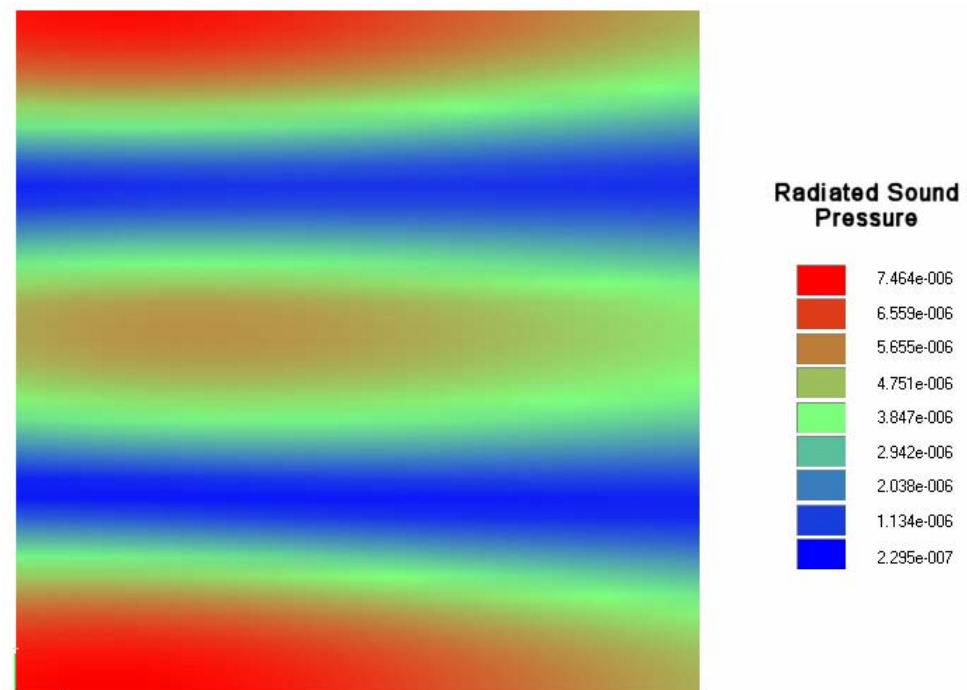


*Figure 2.26 . Manta\_545Hz\_0e-3Damping*

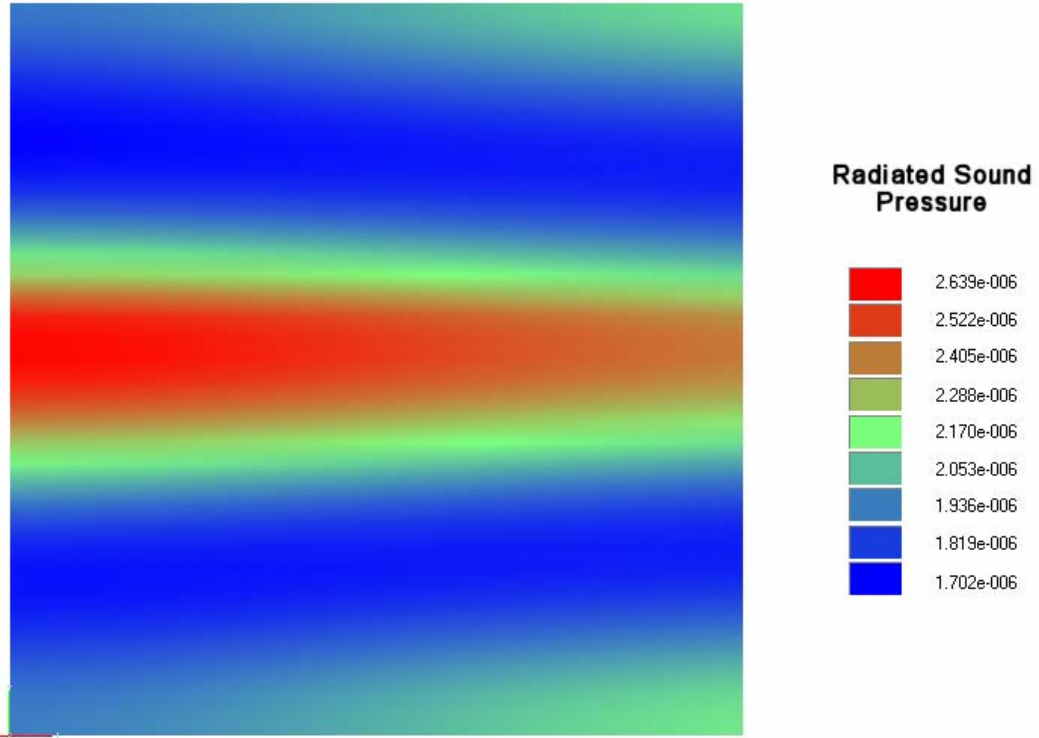


*Figure 2.27 . Manta\_615Hz\_0e-3Damping*

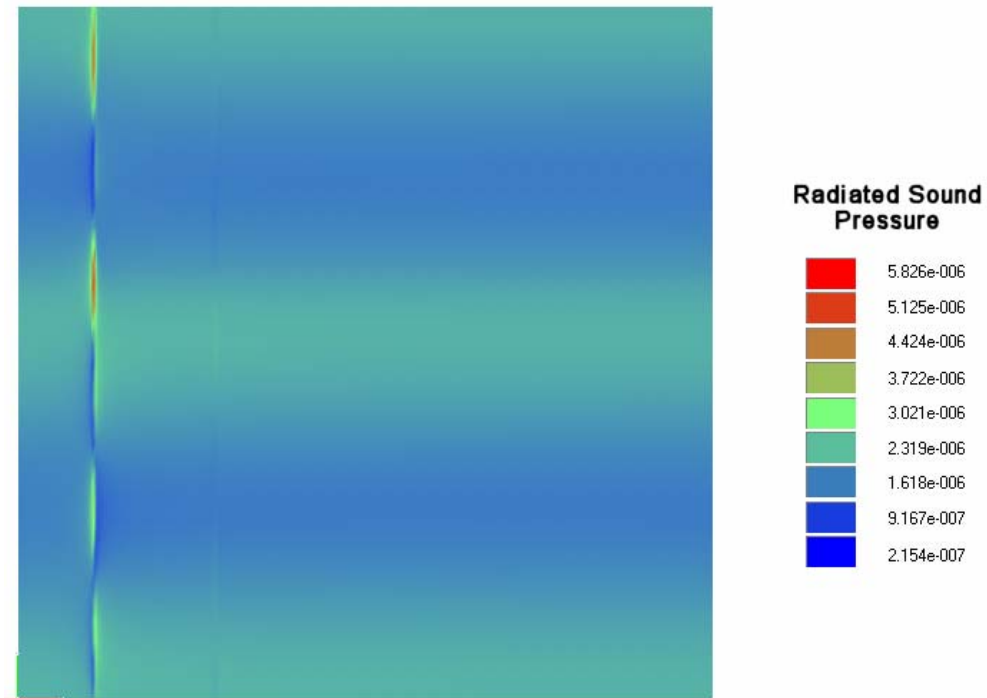


*Figure 2.28 . Manta\_660Hz\_0e-3Damping*

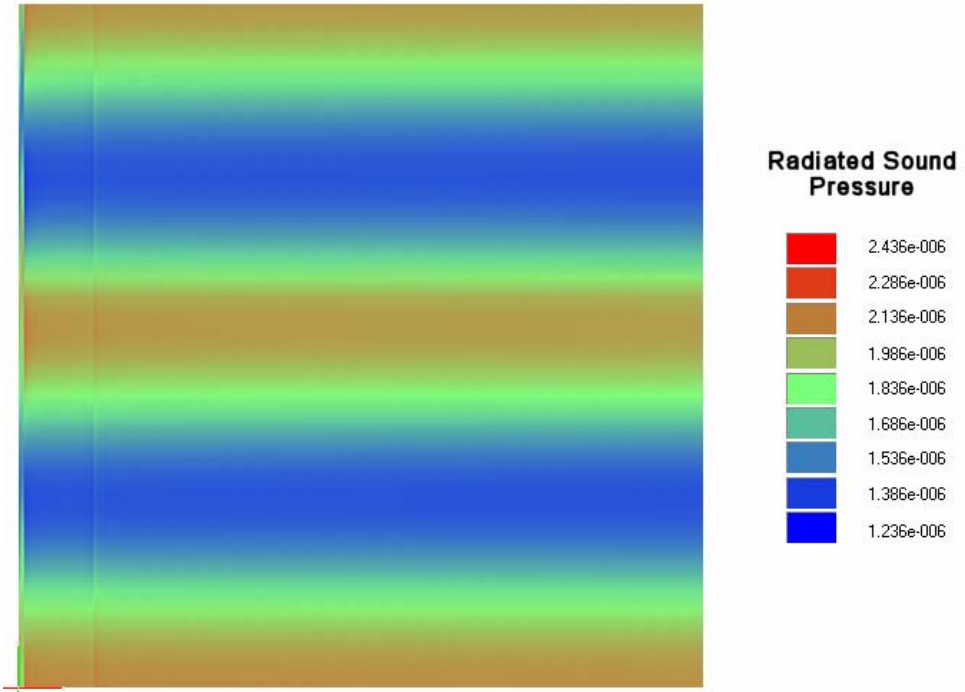


*Figure 2.29 . Manta\_699Hz\_0e-3Damping*

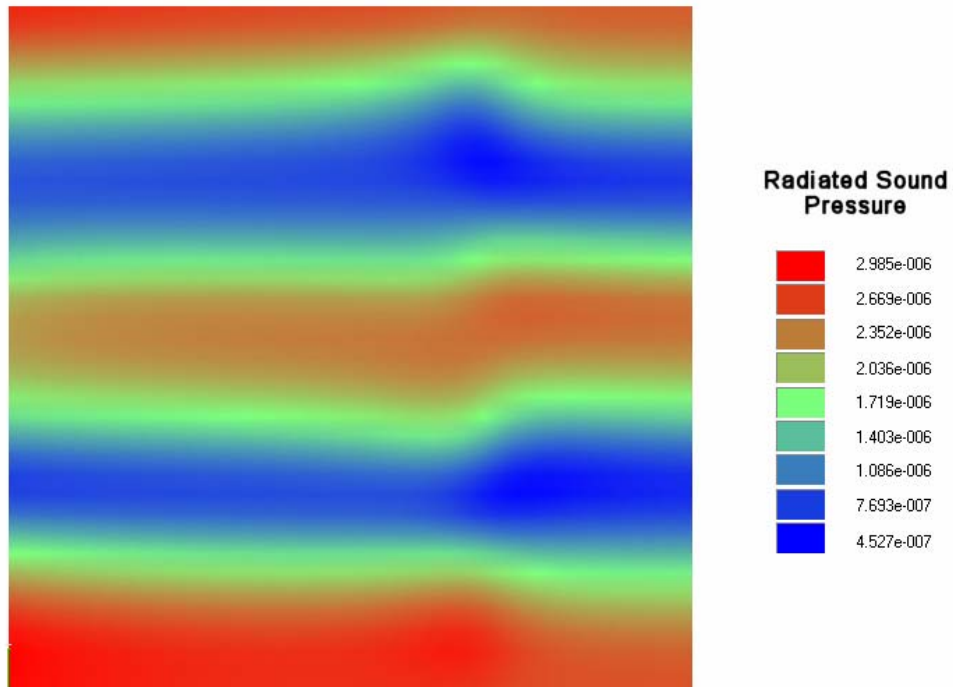


*Figure 2.30 . Manta\_895Hz\_0e-3Damping*

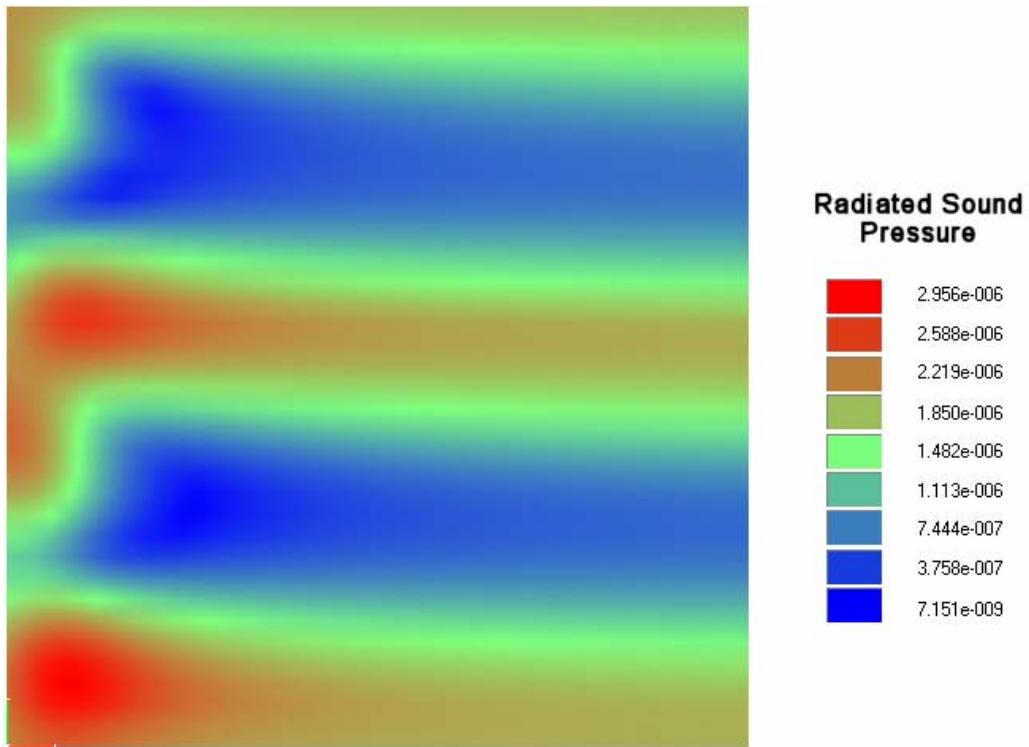


Figure 2.31 . Manta\_900Hz\_0e-3Damping

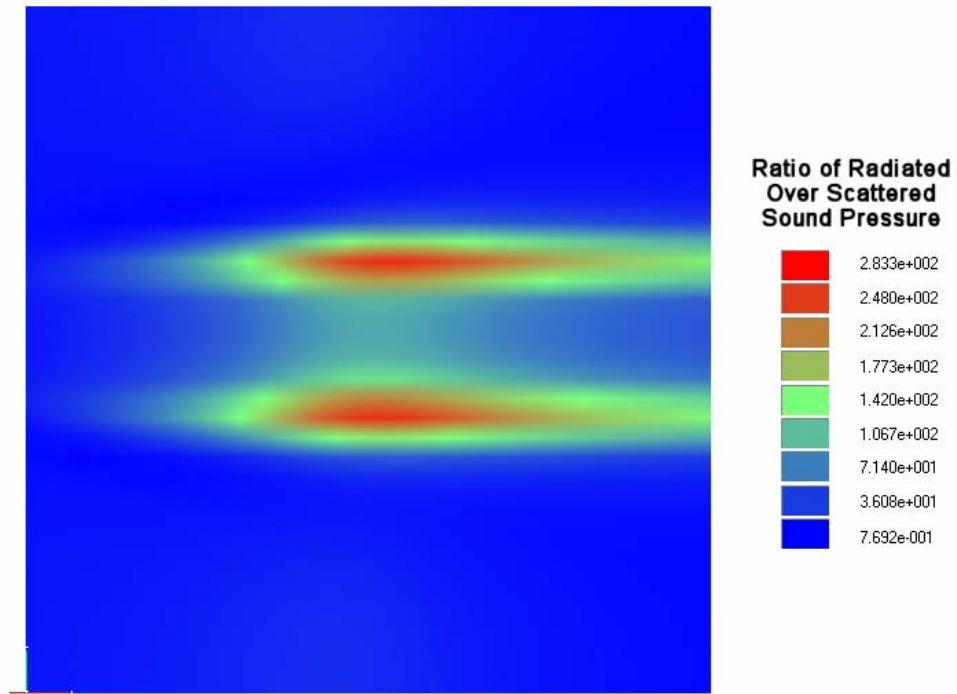


Figure 2.32 . Manta\_365Hz\_0e-3Damping.RAT

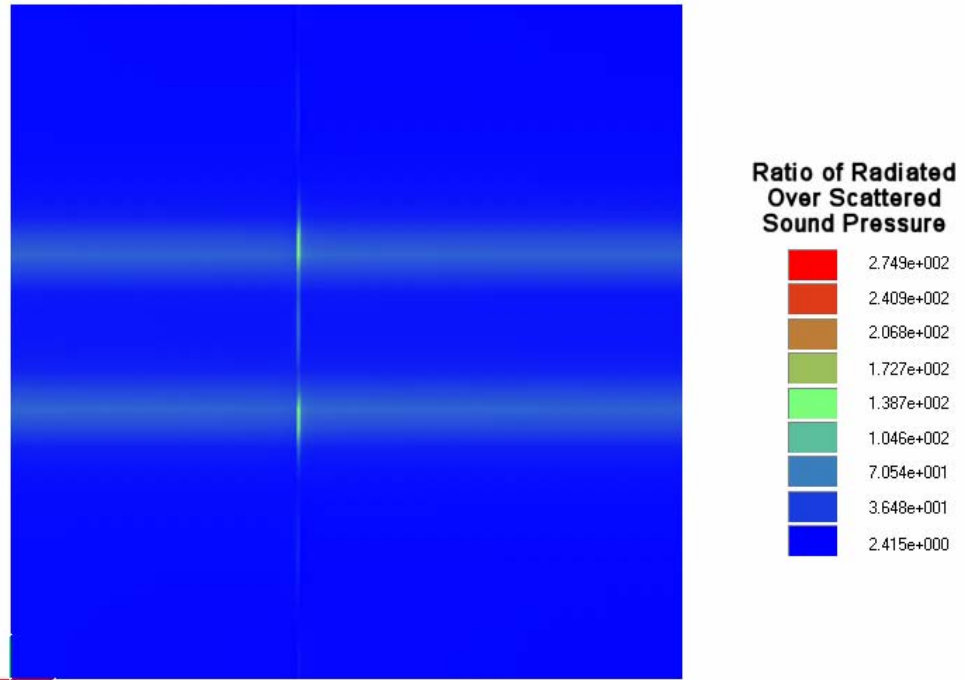


Figure 2.33 . Manta\_379Hz\_0e-3Damping.RAT

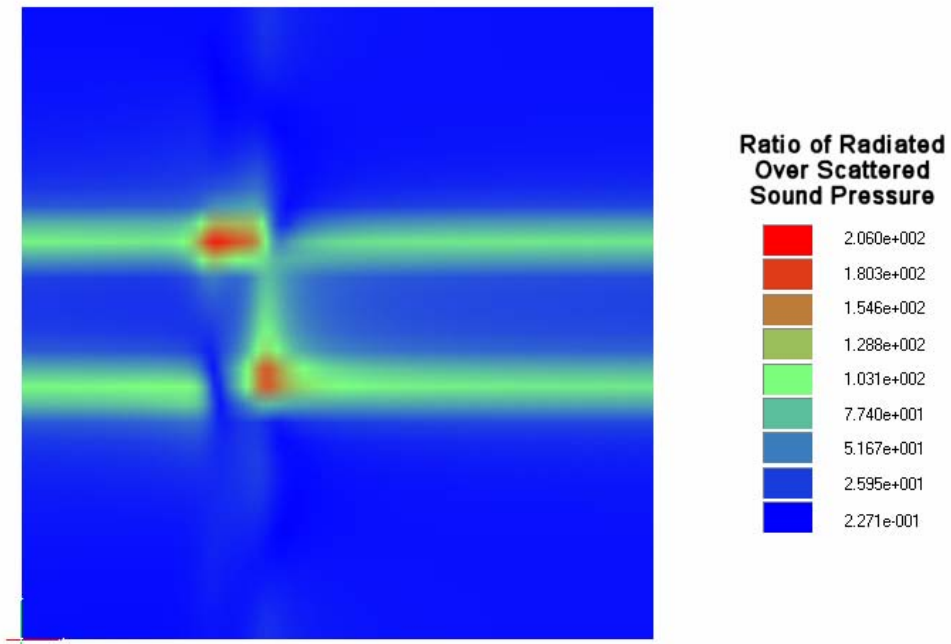


Figure 2.34 . Manta\_396Hz\_0e-3Damping.RAT

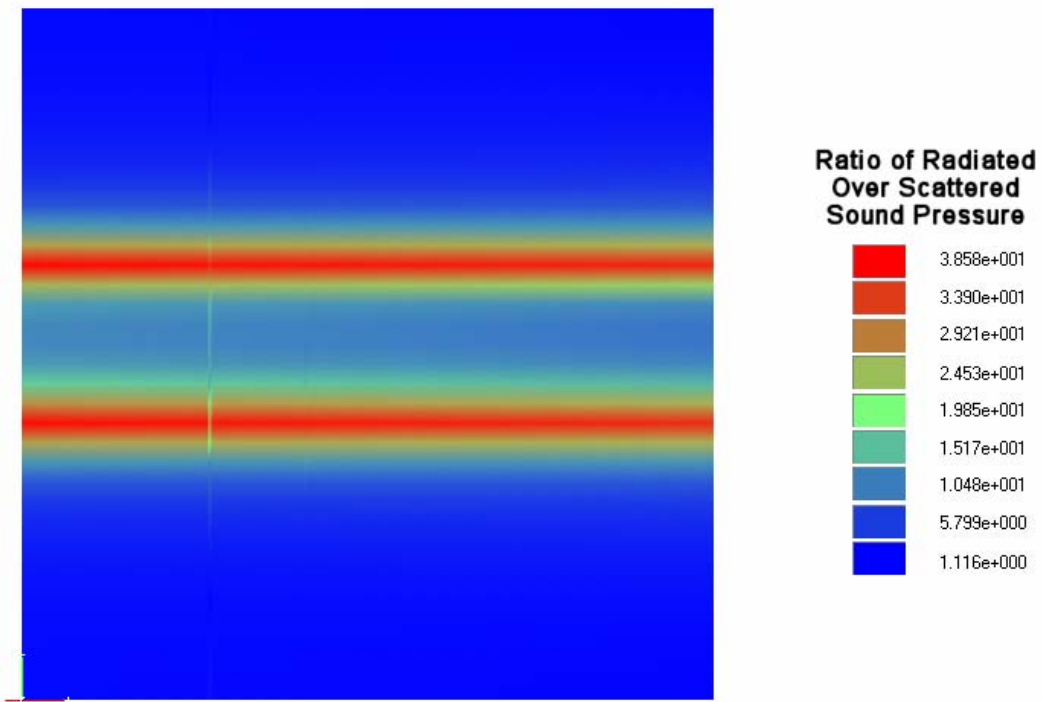


Figure 2.35 . Manta\_419Hz\_0e-3Damping.RAT

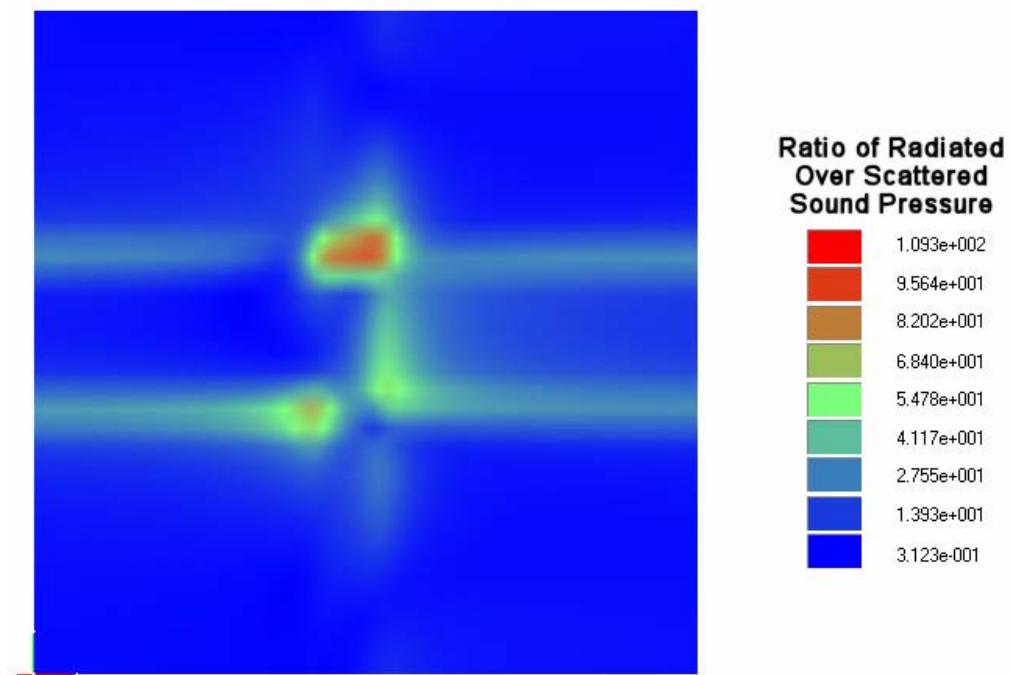
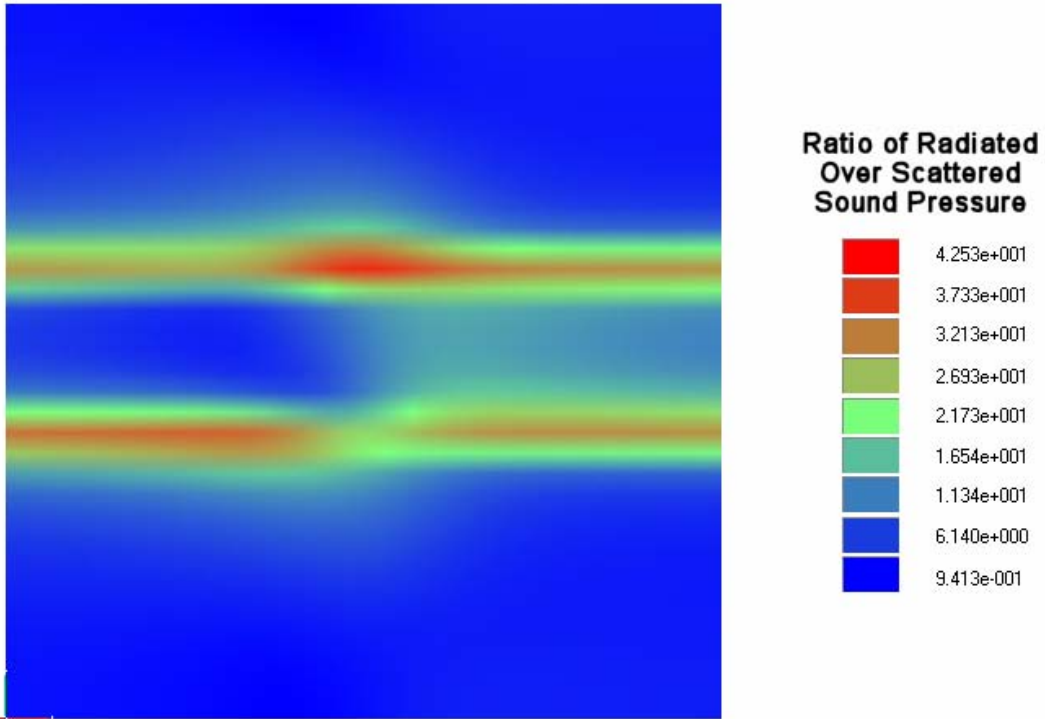
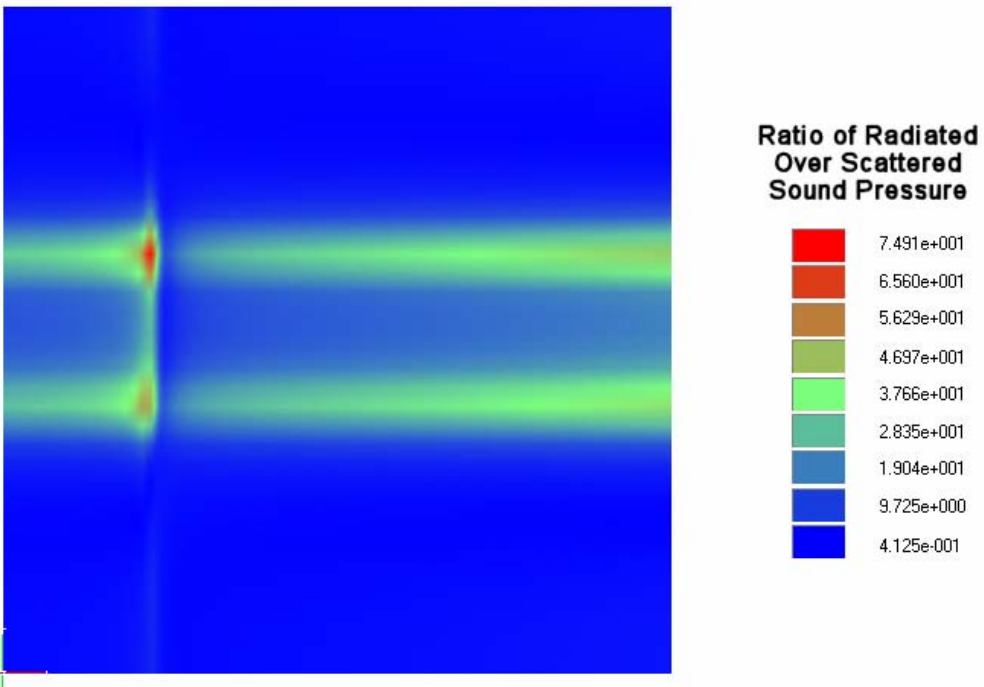


Figure 2.36 . Manta\_434Hz\_2e-3Damping.RAT



*Figure 2.37 . Manta\_434Hz\_5e-3Damping.RAT*



*Figure 2.38 . Manta\_532Hz\_0e-3Damping.RAT*

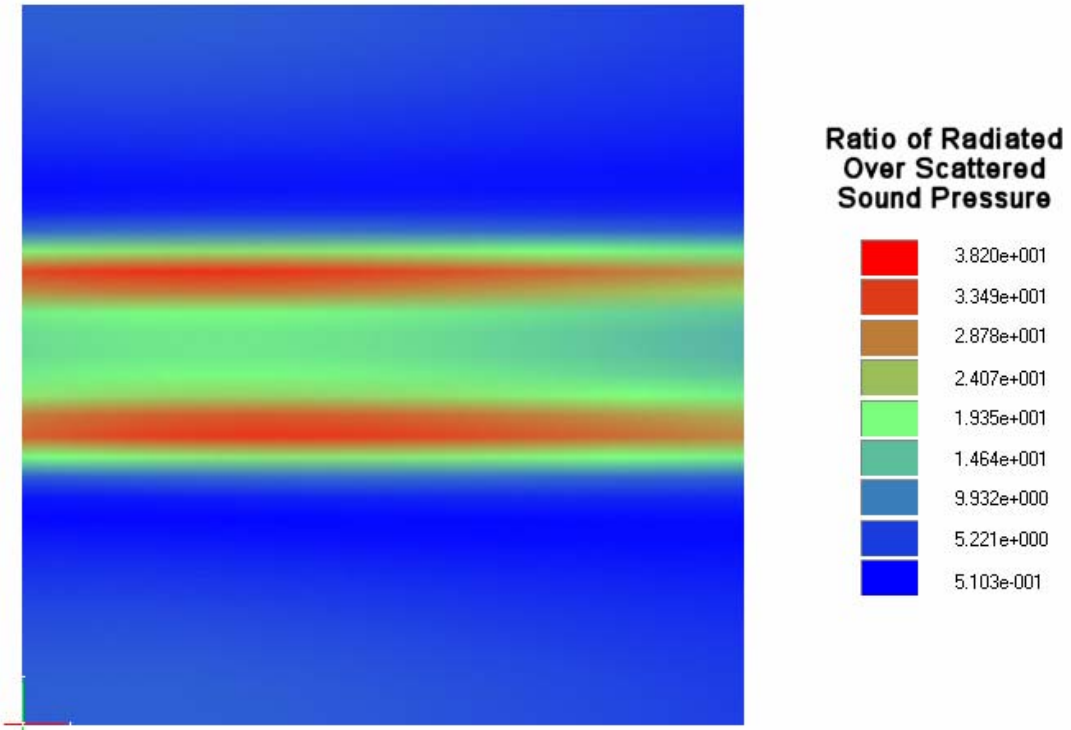


Figure 2.39 . Manta\_545Hz\_0e-3Damping.RAT

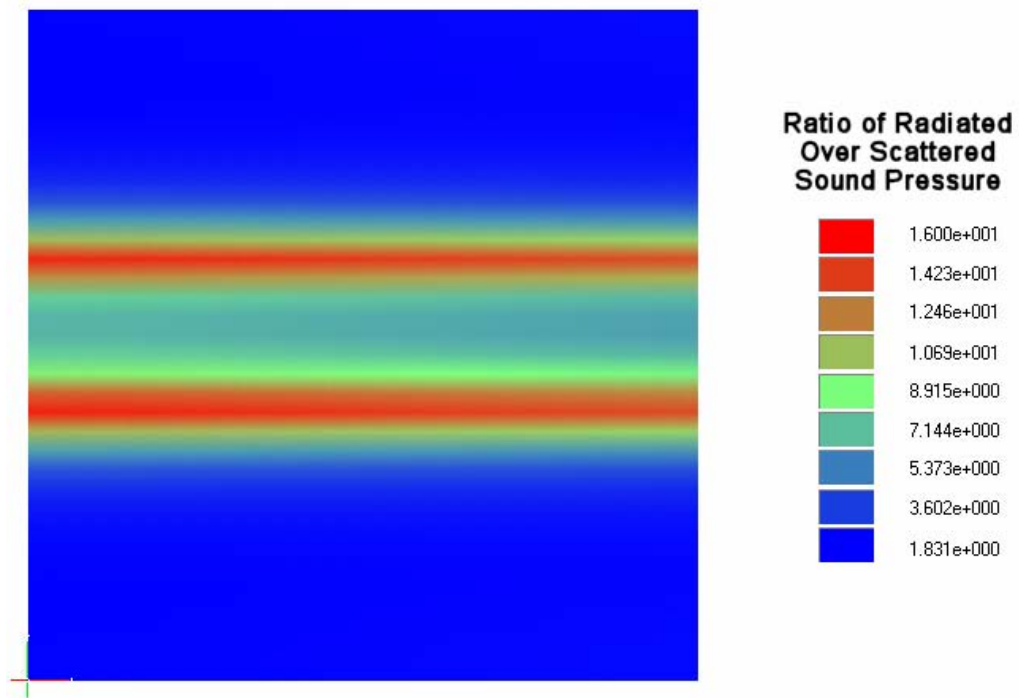


Figure 2.40 . Manta\_615Hz\_0e-3Damping.RAT

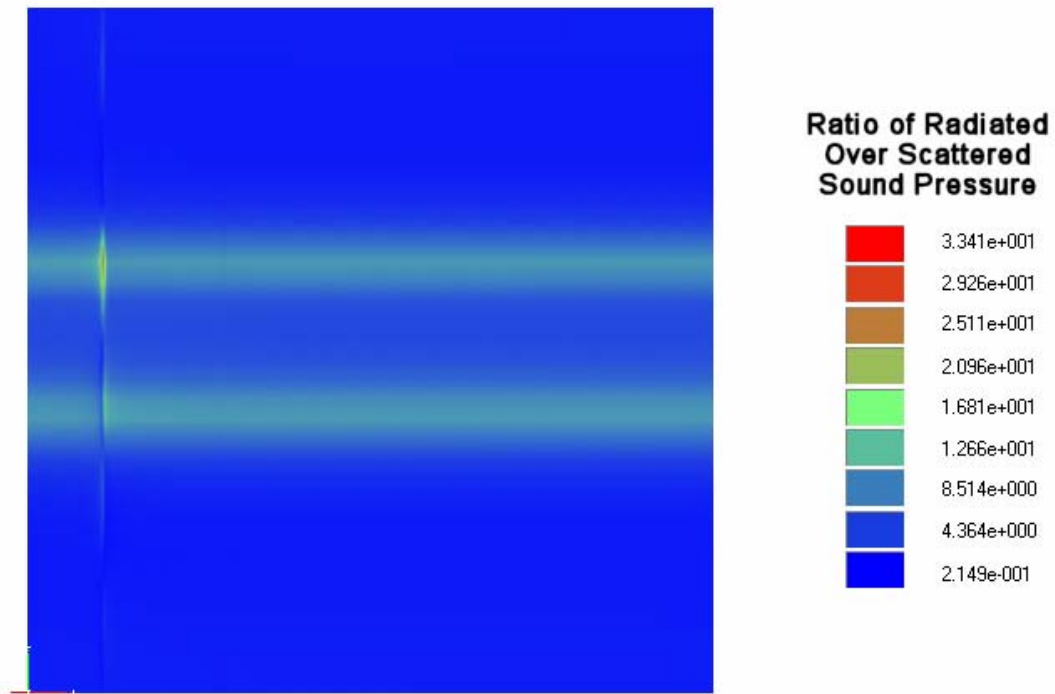


Figure 2.41 . Manta\_660Hz\_0e-3Damping.RAT

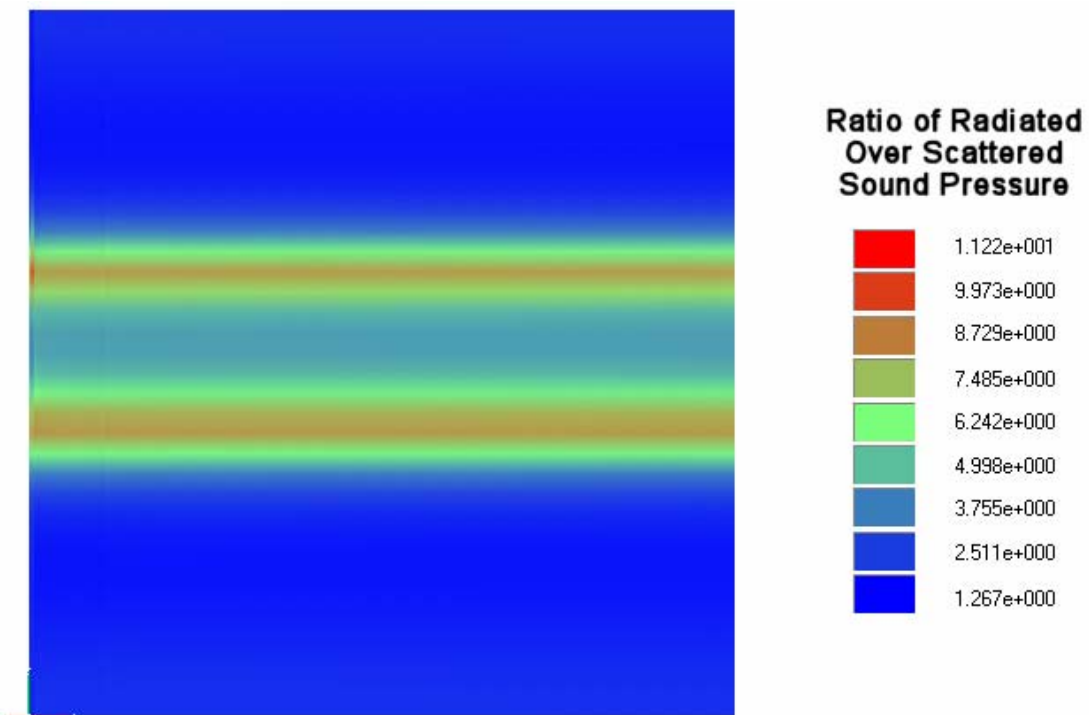


Figure 2.42 . Manta\_699Hz\_0e-3Damping.RAT

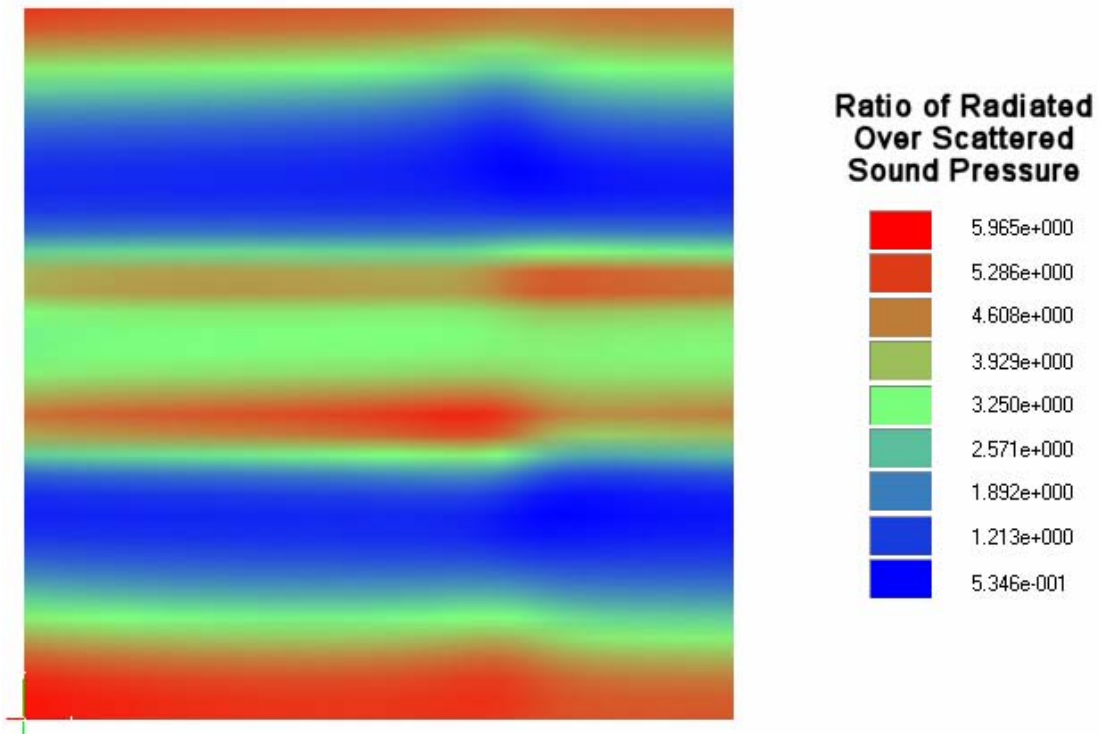


Figure 2.43 . Manta\_895Hz\_0e-3Damping.RAT

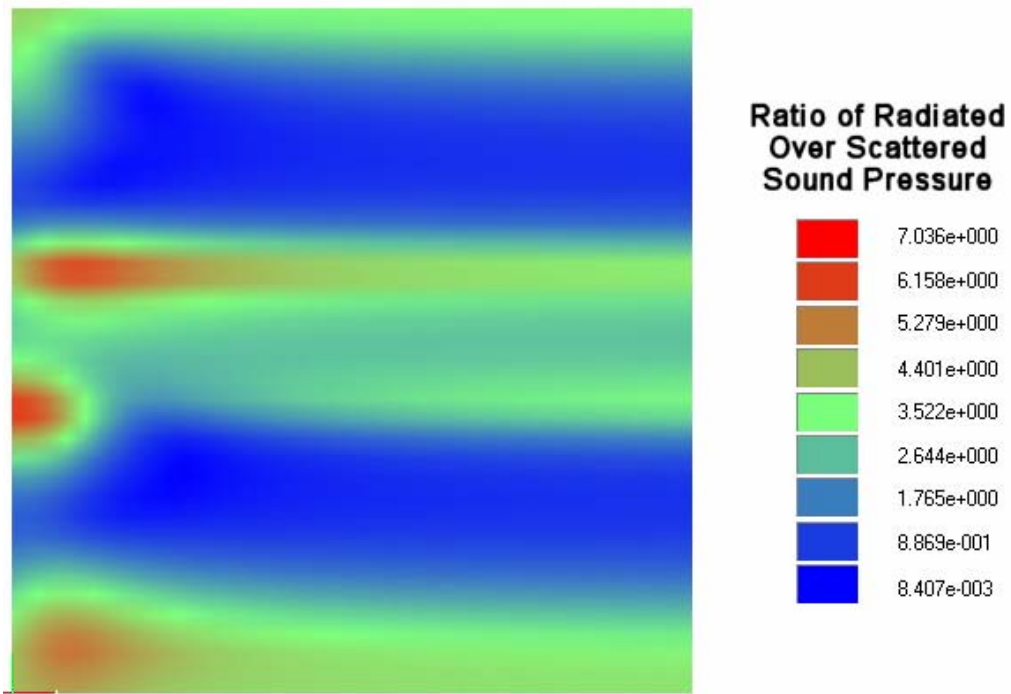
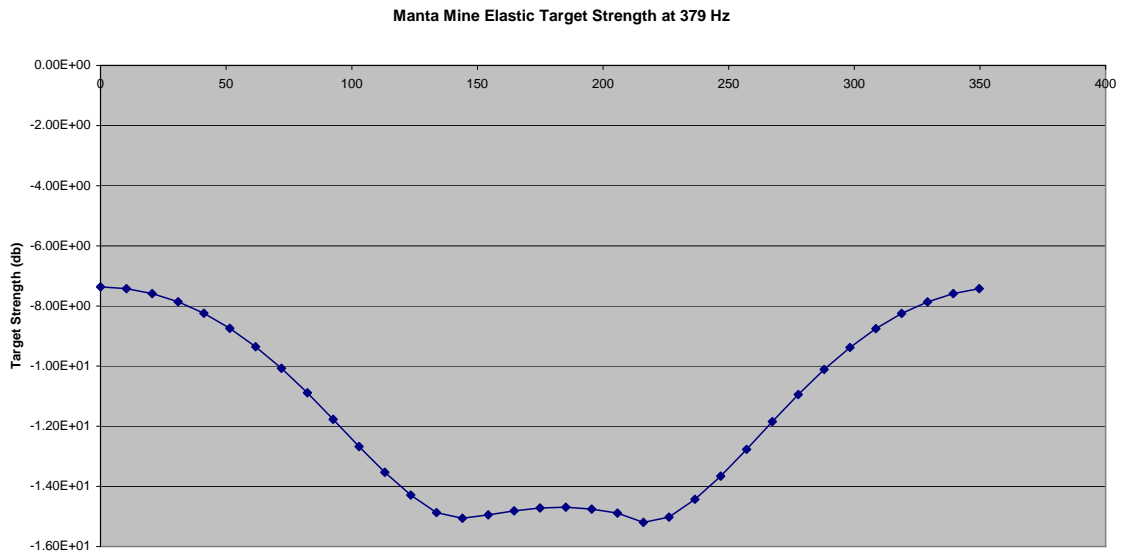
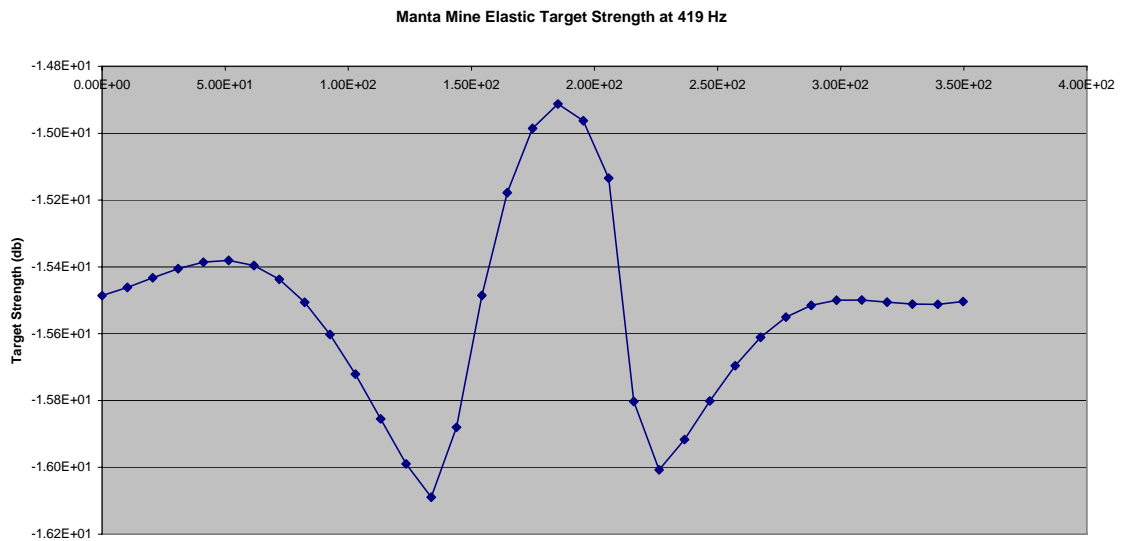


Figure 2.44 . Manta\_900Hz\_0e-3Damping.RAT



**Figure 2.45 . Manta Shape Monostatic Elastic Target Strength at 379 Hz**



**Figure 2.46 . Manta Shape Monostatic Elastic Target Strength at 419 Hz**

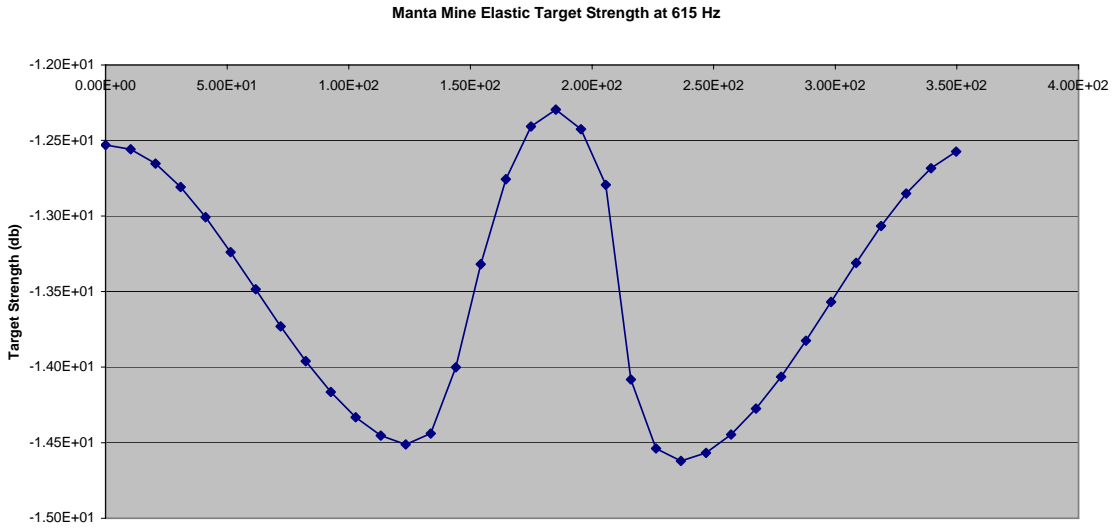


**Figure 2.47 . Manta Shape Monostatic Elastic Target Strength at 616 Hz**

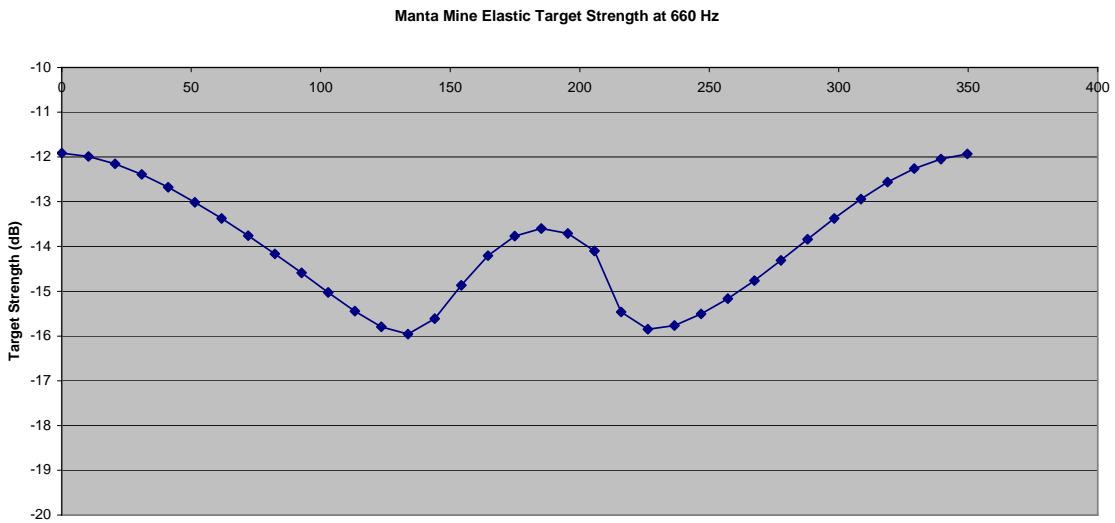


**Figure 2.48 . Manta Shape Monostatic Elastic Target Strength at 660 Hz**

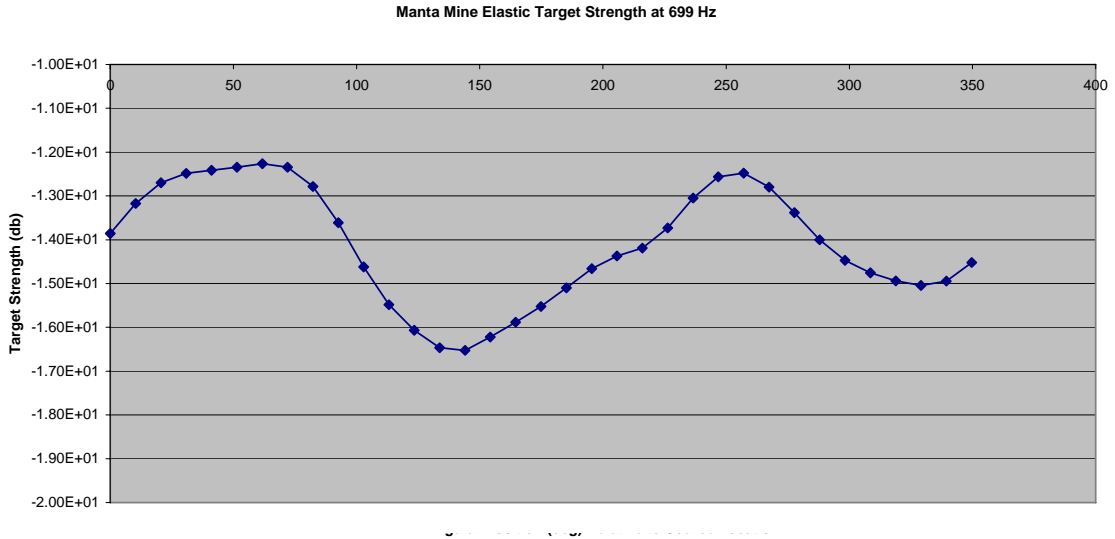


Figure 2.49 . Manta Shape Monostatic Elastic Target Strength at 699 Hz

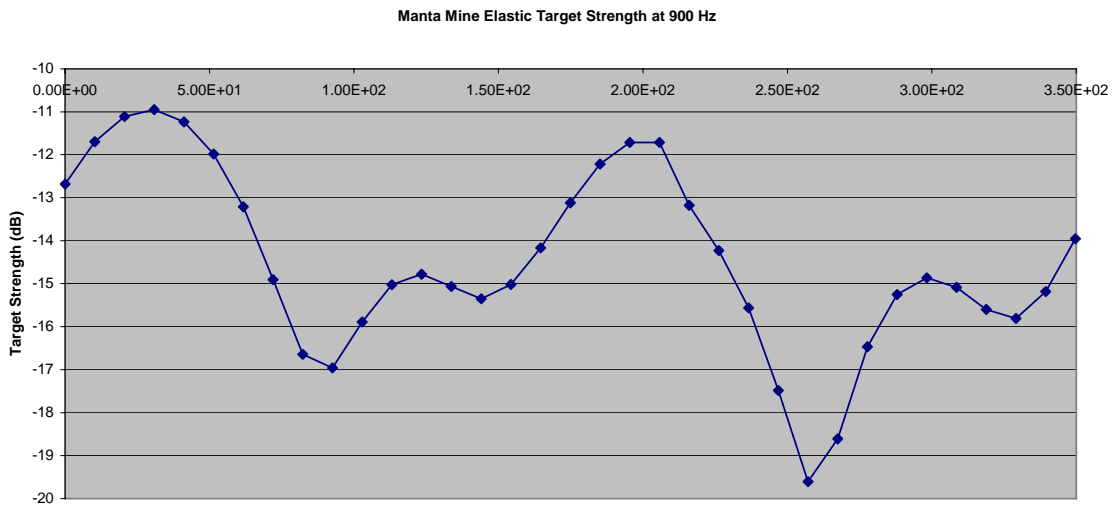


Figure 2.50 . Manta Shape Monostatic Elastic Target Strength at 900 Hz

### 3. Upgrade the AVAST Boundary Element Surface Panel Integration Routines

---

During a recent series of numerical trials, it was found that the numerical integration algorithms developed for use in AVAST were not capable of maintaining a high level of accuracy for extremely thin bodies. This behavior was first identified in simulations involving ship structures having highly tapered bows (see Figure 3.1 as an example). An investigation into the cause of this loss of accuracy determined that the numerical integration routines used to generate the matrix coefficients used in the boundary element models were not well-suited for evaluating the nearly-singular nature of these coefficients. This nearly-singular nature occurs when the centroids of two adjacent panels are separated by a relatively small distance (relative in comparison to the dimensions of the panels).

In order to correct this problem, a semi-analytic approach (based on the Hess-Smith method – see [1]) has been developed and implemented into the latest version of the AVAST code. This new approach is capable of computing matrix coefficients for models having very thin or even collapsed edges.

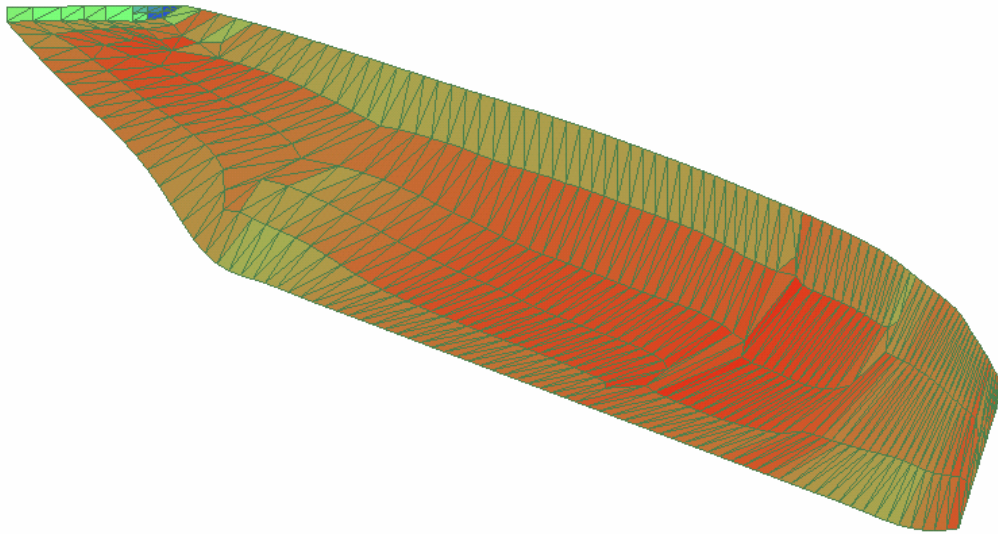


*Figure 3.1 . Sample Boundary Element Mesh for a Ship Hull*

## 4. Upgrade Kirchhoff Scattering Capability

During the previous AVAST development contract, a version of the Kirchhoff scattering algorithm was implemented in the AVAST software. While target strength predictions generated using this algorithm appear to agree closely with other codes, the current AVAST formulation does not account for free surface/shallow water effects or reflections from adjacent structure. The purpose of the current research work is to address these modeling deficiencies and produce an enhanced version of the Kirchhoff scattering algorithm in an upgraded version of the AVAST code. Details related to this work are provided in the discussion which follows.

### 4.1 Free Surface – Shallow Water Effects

In order to account for the effects of free surfaces, rigid surfaces and shallow water fluid domains, a formulation based on the method of images [2] has been incorporated into the latest version of the AVAST code. A similar formulation has been employed in AVAST to model low frequency acoustic radiation and scattering via the Helmholtz equation. In cases involving free or rigid surfaces, a single “mirror” image of the body is placed on the opposite side of the boundary. By positioning an image in this way, the boundary condition on the boundary (i.e., pressure equals zero, or velocity equals zero) is automatically satisfied. A similar technique is used for shallow water fluid domains; however, a series of images must be used (see reference [3]).

Fortunately, only minor changes were needed to upgrade the AVAST code in order to provide this new modeling option. In fact, the bulk of the effort was spent modifying the pre-existing Kirchhoff integral formulation (see Equation 4.1) in order to account for the effects of the secondary images (see Equations 4.2-4.4).

Infinite fluid domain:

$$p_{scat}(P) = \frac{-ik}{4\pi} \oint_s \frac{e^{-ikR_{PQ}}}{R_{PQ}} p_{inc}(Q) [\cos(\phi_{scat}) + \cos(\phi_{inc})] dS_Q \quad (4.1)$$

Half fluid domain with free surface:

$$p_{scat}(P) = \frac{-ik}{4\pi} \oint_s \left( \frac{e^{-ikR_{PQ}}}{R_{PQ}} - \frac{e^{-ik\bar{R}_{PQ}}}{\bar{R}_{PQ}} \right) p_{inc}(Q) [\cos(\phi_{scat}) + \cos(\phi_{inc})] dS_Q \quad (4.2)$$

Half fluid domain with rigid surface:

$$p_{scat}(P) = \frac{-ik}{4\pi} \oint_s \left( \frac{e^{-ikR_{PQ}}}{R_{PQ}} + \frac{e^{-ik\bar{R}_{PQ}}}{\bar{R}_{PQ}} \right) p_{inc}(Q) [\cos(\phi_{scat}) + \cos(\phi_{inc})] dS_Q \quad (4.3)$$

Shallow water (waveguide) fluid domain of depth  $h$ :

$$p_{scat}(P) = \frac{-ik}{4\pi} \oint_s \left( \sum_{n=1}^m G(k, p, q, h, n) \right) p_{inc}(Q) [\cos(\phi_{scat}) + \cos(\phi_{inc})] dS_Q \quad (4.4)$$

where  $P$  represents the position of the field point,  $Q$  represents the location of the centroid of the surface panel,  $k$  represents the acoustic wavenumber,  $R_{PQ}$  represents the distance between the field point and surface panel,  $\bar{R}_{PQ}$  represents the distance between the field point and image surface panel,  $p_{inc}(Q)$  represents the magnitude of the incident pressure at the surface panel  $Q$ , and  $\phi_{scat}$  and  $\phi_{inc}$  are assumed to represent the angle between the surface normal and the vectors representing relative position of the field and source points with respect to panel centroid.

## 4.2 Multiple Reflections

In order to account for multiple reflections, the pre-existing AVAST Kirchhoff formulation was modified so that the scattering pressure computed on the surface of the boundary element panels would be modeled as secondary source terms. In terms of the AVAST formulation, given the particular type of fluid domain, one of the four equations provided above would be used to compute the scattered pressure contribution made by source at the various field locations. This contribution is considered the “primary” source term. Once this primary contribution has been computed, then the contributions made by secondary reflections coming from the individual panels are computed. For these secondary reflections, the location of the source is moved to centroids of the individual panels, and the strength of the source is set equal to the scattered pressure computed for the panel centroid. As a result, for an infinite fluid domain, Equation (4.1) is solved once using the strength and location of the primary source term, and then repeated once for each surface panel, this time using the location of the panel centroid and the strength of the scattered pressured at this location to serve as the secondary source.

## 4.3 Example

In order to demonstrate the capabilities of the newly upgraded AVAST Kirchhoff scattering modeling capability, consider the model of boundary element model of a

generic submarine sail provided below in Figure 4.1 [4]. For the purposes of this study, target strength predictions have been made for two model configurations: the sail at a depth of 3.0m and at a depth of 300m. For the 300m case, the fluid domain was assumed to be infinite in extent. Figure 4.2 provides a comparison of the target strength predictions made by newly upgraded AVAST code. As expected, the target strength changes significantly (increasing particularly close to broadside (90°)) as the sail approaches the free surface.

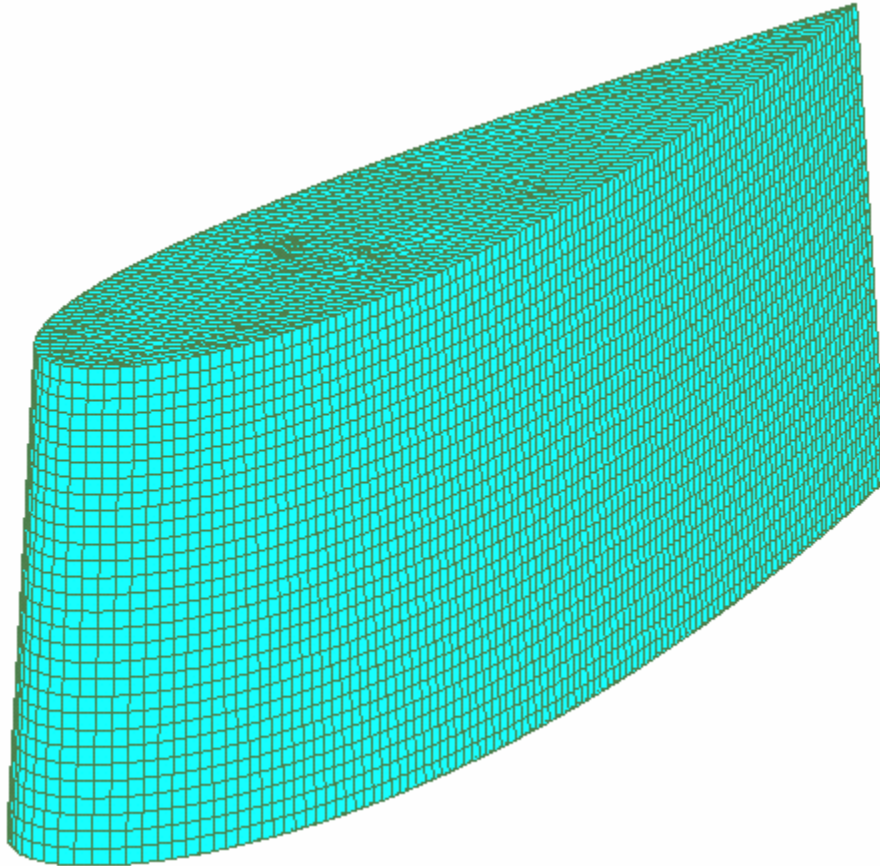


**Figure 4.1. Generic Submarine Sail Model**

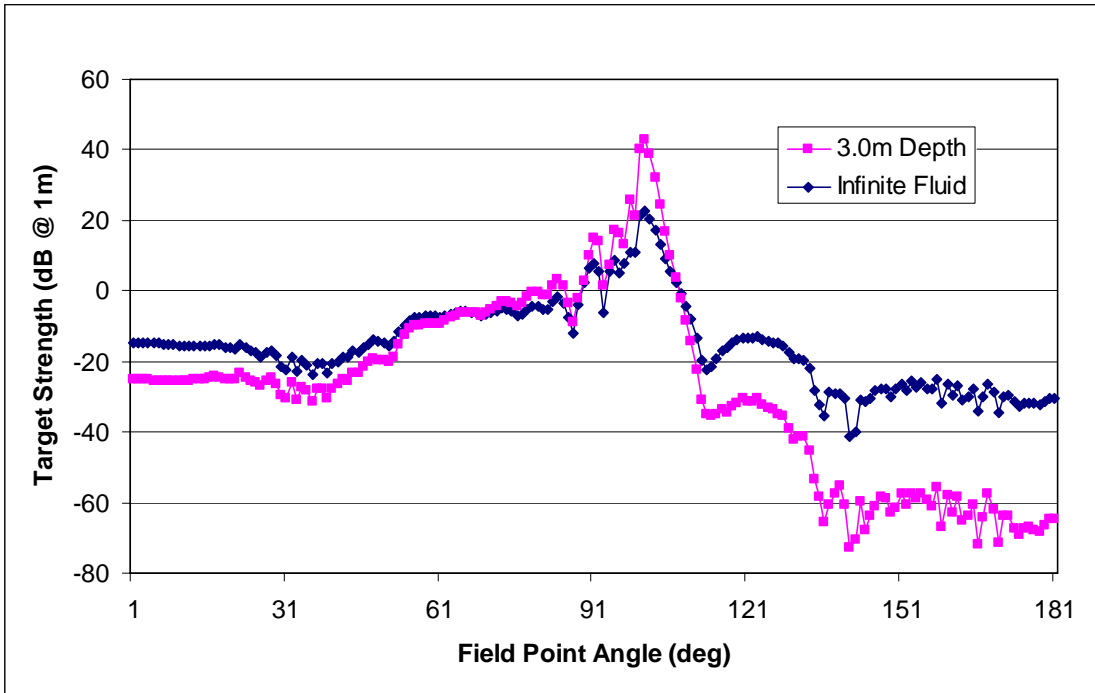


**Figure 4.2. A Comparison of Target Strength Predictions for Submarine Sail at 4 kHz (infinite Fluid vs a Free Surface Height 3m Above the Top of the Sail)**

## 5. References

---

1. K.J. Bathe, Finite Element Procedures in Engineering Analysis, Prentice-Hall, Inc., Englewood Cliffs, NJ, 1982
2. J.A. Fawcett, "Modeling of High Frequency Scattering From Objects Using a Hybrid Kirchhoff/Diffraction Approach", J.A.S.A., 109 (4), April 2001.
3. K.G. Foote, "Comparing Kirchhoff Approximation and Boundary Element Models for Computing Gadoid Target Strengths", J.A.S.A., 111 (4), April 2002.
4. H.G. Schneider, et. al., "Acoustic Scattering by a Submarine: Results from a Benchmark Target Strength Simulation Workshop", Tenth International Congress on Sound and Vibration, Stockholm, Sweden, July, 2003.

This page intentionally left blank.

## Distribution list

---

### A. INTERNAL

1 Author  
5 Library

### B. EXTERNAL

#### **National Defence Headquarters**

MGen. George R. Pearkes Bldg.  
101 Colonel By Drive  
Ottawa, Ontario  
K1A 0K2

1 DRDKIM  
1 DMSS 2

8 TOTAL

This page intentionally left blank.

<b>DOCUMENT CONTROL DATA</b>		
(Security classification of title, body of abstract and indexing annotation must be entered when the overall document is classified)		
<p>1. <b>ORIGINATOR</b> (the name and address of the organization preparing the document. Organizations for whom the document was prepared, e.g. Centre sponsoring a contractor's report, or tasking agency, are entered in section 8.)</p> <p><b>Martec Limited 1888 Brunswick Street, Suite 400 Halifax, Nova Scotia B3J 3J8</b></p>	<p>2. <b>SECURITY CLASSIFICATION</b> (overall security classification of the document including special warning terms if applicable).</p> <p><b>UNCLASSIFIED</b></p>	
<p>3. <b>TITLE</b> (the complete document title as indicated on the title page. Its classification should be indicated by the appropriate abbreviation (S,C,R or U) in parentheses after the title).</p> <p><b>Further Enhancements To The High Frequency Target Strength Prediction Capabilities Of AVAST</b></p>		
<p>4. <b>AUTHORS</b> (Last name, first name, middle initial. If military, show rank, e.g. Doe, Maj. John E.)</p> <p><b>D.P. Brennan</b></p>		
<p>5. <b>DATE OF PUBLICATION</b> (month and year of publication of document)</p> <p><b>August 2007</b></p>	<p>6a. <b>NO. OF PAGES</b> (total containing information Include Annexes, Appendices, etc).</p> <p><b>48</b></p>	<p>6b. <b>NO. OF REFS</b> (total cited in document)</p> <p><b>4</b></p>
<p>7. <b>DESCRIPTIVE NOTES</b> (the category of the document, e.g. technical report, technical note or memorandum. If appropriate, enter the type of report, e.g. interim, progress, summary, annual or final. Give the inclusive dates when a specific reporting period is covered).</p> <p><b>CONTRACT REPORT</b></p>		
<p>8. <b>SPONSORING ACTIVITY</b> (the name of the department project office or laboratory sponsoring the research and development. Include address).</p> <p><b>Defence R&amp;D Canada – Atlantic PO Box 1012 Dartmouth, NS, Canada B2Y 3Z7</b></p>		
<p>9a. <b>PROJECT OR GRANT NO.</b> (if appropriate, the applicable research and development project or grant number under which the document was written. Please specify whether project or grant).</p> <p><b>Project 11cj</b></p>	<p>9b. <b>CONTRACT NO.</b> (if appropriate, the applicable number under which the document was written).</p> <p><b>W7707-03-2334</b></p>	
<p>10a. <b>ORIGINATOR'S DOCUMENT NUMBER</b> (the official document number by which the document is identified by the originating activity. This number must be unique to this document.)</p> <p><b>DRDC Atlantic CR 2007-216</b></p>	<p>10b. <b>OTHER DOCUMENT NOS.</b> (Any other numbers which may be assigned this document either by the originator or by the sponsor.)</p> <p><b>N/A</b></p>	
<p>11. <b>DOCUMENT AVAILABILITY</b> (any limitations on further dissemination of the document, other than those imposed by security classification)</p> <p>( <input checked="" type="checkbox"/> ) Unlimited distribution  ( ) Defence departments and defence contractors; further distribution only as approved  ( ) Defence departments and Canadian defence contractors; further distribution only as approved  ( ) Government departments and agencies; further distribution only as approved  ( ) Defence departments; further distribution only as approved  ( ) Other (please specify):</p>		
<p>12. <b>DOCUMENT ANNOUNCEMENT</b> (any limitation to the bibliographic announcement of this document. This will normally correspond to the Document Availability (11). However, where further distribution (beyond the audience specified in (11) is possible, a wider announcement audience may be selected).</p> <p><b>Full, unlimited</b></p>		

13. **ABSTRACT** (a brief and factual summary of the document. It may also appear elsewhere in the body of the document itself. It is highly desirable that the abstract of classified documents be unclassified. Each paragraph of the abstract shall begin with an indication of the security classification of the information in the paragraph (unless the document itself is unclassified) represented as (S), (C), (R), or (U). It is not necessary to include here abstracts in both official languages unless the text is bilingual).

The development and incorporation of the latest enhancements to the AVAST code are described. The purpose of this work was to make the modeling of the physical environment more realistic, while ensuring that the code runs as efficiently as possible. To this end several new features have been added. These include modifying the high-frequency Kirchhoff scattering method in order to allow for at least one reflection and upgrading the existing boundary element surface panel integration routines. The contract also addresses the need to investigate the high frequency target strength of Manta shapes.

14. **KEYWORDS, DESCRIPTORS or IDENTIFIERS** (technically meaningful terms or short phrases that characterize a document and could be helpful in cataloguing the document. They should be selected so that no security classification is required. Identifiers, such as equipment model designation, trade name, military project code name, geographic location may also be included. If possible keywords should be selected from a published thesaurus. e.g. Thesaurus of Engineering and Scientific Terms (TEST) and that thesaurus-identified. If it not possible to select indexing terms which are Unclassified, the classification of each should be indicated as with the title).

AVAST  
Finite element method  
Boundary integral equation method  
Acoustics  
Target strength  
Kirchhoff  
mine

This page intentionally left blank.

## **Defence R&D Canada**

Canada's leader in defence  
and National Security  
Science and Technology

## **R & D pour la défense Canada**

Chef de file au Canada en matière  
de science et de technologie pour  
la défense et la sécurité nationale



[www.drdc-rddc.gc.ca](http://www.drdc-rddc.gc.ca)